Investigation of Implantable Multichannel Neurostimulators

by

Yashwanth Nanda Kumar

A Thesis Presented in Partial Fulfillment
of the Requirements for the Degree
Master of Science

Approved July 2015 by the
Graduate Supervisory Committee:

Bruce Towe, Chair
Jitendran Muthuswamy
Mehdi Nikkhah

ARIZONA STATE UNIVERSITY

August 2015

ABSTRACT

There is a strong medical need and important therapeutic applications for improved wireless bioelectric interfaces to the nervous system. Multichannel devices are desired for neural control of robotic prosthetics that interface to remaining nerves in limb stumps of amputees and as alternatives to traditional wired arrays used in for some types of brain stimulation. This present work investigates a new approach to ultrasound-powering of implantable microelectronic devices within the tissue that may better support such applications. These devices are of ultra-miniature size that is enabled by a wireless technique. This study investigates two types of ultrasound-powered neural interfaces for multichannel sensory feedback in neurostimulation. The piezoceramics lead zirconate titanate (PZT) ceramic and polyvinylidene fluoride (PVDF) polymer were the primary materials used to build the devices. They convert ultrasound to electricity that when rectified by a diode produce a current output that is neuro stimulatory to peripheral nerve or the neurons in the brain. Multichannel devices employ a form of spatial multiplexing that directs focused ultrasound towards localized and segmented regions of PVDF or PZT that allows independent channels of nerve actuation. Different frequencies of ultrasound were evaluated for best results. Firstly, a 2.25 MHz frequency signal that is reasonably penetrating through body tissue to an implant several centimeters deep and also a 5 MHz frequency more suited to application for actuation of devices within a less than a centimeter of nerve. Results show multichannel device performance to have a complex inter-relationship with frequency, size and thickness, angular incidence, channel separations, and number of folds (layers connected in series and parallel). The output electrical port impedances of PVDF devices were examined in relationship to that of stimulating electrodes and tissue interfaces. Miniature multichannel devices were constructed using an unreported method of employing state of the art laser cutting systems. The results show that PVDF based devices have advantages over PZT, because of better acoustic coupling with tissue, known better biocompatibility, and better separation between multiple channels. However, the PZT devices proved to be better overall in terms of compactness and higher outputs for a given ultrasound power level.

DEDICATION

As Steve Jobs once said “You can't connect the dots looking forward; you can only connect them looking backwards. So you have to trust that the dots will somehow connect in your future.” I have finally connected the dots to successfully finish this thesis.

I dedicate this work to my parents, who were my pillars of strength. From the day I held on to a slate to learn the alphabets till today, they have been with me guiding and watching my progress;

Nanda Kumar Balakrishnan and Madhuri Nanda Kumar, this is all because of the sacrifices you both made all through.

Also, my Grandfather Balakrishnan Govindaswamy. You had done some unbelievable things in the past. Right from taking photocopies of my answer sheets where I scored a centum to being an aide in all my academic adventures. Constantly telling me to read daily to learn something new and try doing it differently. You taught me the skill of picking up things lying around and make something working out of it. I hope you are watching me from up above when I am defending and getting my Master’s degree.

ACKNOWLEDGMENTS

I would like to thank Dr. Bruce Towe for giving me the opportunity to explore such a challenging thesis, providing me constant guidance to make sure I completed the work required. An extended thanks to Dr. Jitendran Muthuswamy for generously agreeing to let me use his lab resources when needed and being on my committee along with Dr. Mehdi Nikkhah for the completion of this thesis.

I would like to thank Dr. Vincent Pizziconi for allowing me to use the laser systems and other resources at the design studio.

Any work isn't complete without a little help from friends and colleagues. I would also like to extend my sincere thanks to several individuals who played a crucial role in helping me with several experiments and procedures patiently and sometimes kind encouraging words which boosted my morale.

Thanks a lot

Swarnima Pandey

Dan Gulick

Xi Zong

Dmitrijs Celinskis

Ankur Shah

Sanchit Chirania

Ranjani Sampath

Swathy Sampath

Colin Barry

My roomates and close friends.

Project Humanities head Dr. Lester, staff and colleagues for being patient with me and putting up with my work schedules.

Finally, Arizona State University, where all this amazing work took place.

TABLE OF CONTENTS

Page

LIST OF TABLES…….....…….vi

LIST OF FIGURES……..……...……...vii

CHAPTER

1 INTRODUCTION……...…….……....1

2 BACKGROUND……....3

2.1 Functional Electrical Stimulation……...….3

2.2 Electrical Stimulation for the Treatment of Epilepsy……...…4

2.3 Microelectrode Array for Chronic Deep- Brain Microstimulation for Treating Parkinson's Disease…..……..……..4

2.4 Neural Prosthesis……..……..5

2.5 Multielectrode Array for Intrafascicular Recording and Stimulation……5

2.6 Nerve Stimulation: Cathodic and Anodic Stimulation...……..6

2.7 Current Techniques……..6

2.8 Ultrasound Properties and Piezoelectric Effect..…….……...10

2.9 General Description of PVDF And PZT and Their Interaction with Sound……...……..10

2.10 Single Diode Stimulator Theory…….....12

2.11 Conductivity of Different Tissues……..…….……12

3 METHODS .....…….…….14

3.1 Construction of the Neuro Stimulators…….……...14

3.2 Characterization Study of the Piezoelectric Materials……..……15

3.3 Experimental Setup……..……....22

3.4 Experimental Procedure……..…….....26

3.5 Capacitance Measurements of the PVDF and PZT Test Devices……29

3.6 Fabrication of PVDF Based Neurostimulators……..…….…..29

3.7 Capacitance Calculations of PVDF Neurostimulators.…….…….……..34

3.8 Fabrication of PZT Based Neurostimulators……..…..……..35

CHAPTER Page

3.9 Capacitance Calculations of PZT Neurostimulators……..……..41

3.10 Bench Test of Neurostimulators for Maximum Voltage Generated Under Tissue Conductivity……41

3.11 Demonstration of Multichannel Functionality of the Neurostimulators ……..…….44

3.12 Current Generated in the Nickel and Gold Plated 2 Channel Devices……..…45

3.13 Output Dependency of the Devices with Respect to the Conductivity of the Solution……..……45

3.14 Ultrasound Acoustic Power and Focal Spot Experiment to Determine Acoustic Power Density……..…….46

3.15 Impedance Measurements of the Different Electrodes Used: Electrode-Electrolyte Interface…….47

4 RESULTS……..……...…49

4.1 In- Vitro Performance of a Piezoelectric Element to Ultrasound……..…….49

4.2 Bench Tests of PVDF Test Elements…….……..49

4.3 Capacitance of PVDF Test Elements……...……..54

4.4 Bench Tests of PZT Test Elements……...…...54

4.5 Capacitance of the PZT Test Elements…….…..…58

4.6 Bench Test for Devices to Check for Their Maximum Voltages……...……..59

4.7 Demonstration of Multichannel Functionality in PVDF and PZT Neurostimulators……63

4.8 Output Dependence on Conductivity……..…..…..…71

4.9 Impedance Measurements of Different Electrodes……..……..72

4.10 Acoustic Power, Focal Spot and Acoustic Power Density Measurements..……...75

4.11 Wavelengths of the Different Transducers……..……75

4.12 Live Animal Experiments……..……..75

5 DISCUSSION …….....……82

6 CONCLUSION ……..……....88

References……....……...89

LIST OF TABLES

Table Page

1. Summary of the Properties of PZT and PVDF Materials……...12

2. Conductivity of Different Tissues…….....…….13

3. PVDF Device Dimensions…….……29

4. Capacitance of PVDF Test Materials…….……..…….54

5. Capacitance of PZT Test Materials……..……..……..58

6. Short- Pulse Response Bench Test of PVDF Devices……59

7. Tone Burst Bench Test of PVDF Devices……..…….....…...60

8. Capacitance of PVDF Fabricated Devices……....61

9. Short Pulse Bench Test of PZT Devices……...……...……...62

10. Tone Burst Bench Test of PZT Devices……..….....62

11. Wavelength and Half Wavelenghts of the Different Transducers Ultrasound Beams…….....75

LIST OF FIGURES

Figure		Page
1.	Utah Electrode Array System	7
2.	Piezoelectric Effect	10
3.	Piezoelectric Axis	11
4.	Single Diode Stimulator Design	14
5.	An Example of the PVDF Sheet with the Positive Polarity Marked and Cut	16
6.	MG Chemicals Conductive Epoxy	16
7.	Sandwiched PVDF Layers.	17
8.	Heat Lamp Setup to Cure the PVDF Layers	17
9.	Universal Laser Systems(ULS) 40 W Laser Systems	18
10.	PZT Test Materials	19
11.	Pictorial Representation of the Design Process to Print in Adobe Illustrator	20
12.	ULS Print Interface	21
13.	The Test Devices After the Laser Cut Process	22
14.	Panametrics Inc Pulser Receiver Setup	23
15.	Tone Burst Response System Setup	24
16.	Overall Assembly of the Setup	25
17.	Top View of the Setup	25
18.	Tweezer Setup	26
19.	A Fanfold Structure of PVDF Layers	30
20.	Step By Step Illustration of the Whole Process of Making PVDF Series Devices	31
21.	A Representation of the 3 Channel and 4 Channel PVDF Layers	32
22.	Packaged Anodic Stimulation Devices with Series Interconnects	32
23.	Three Layers and Five Layer Devices	33
24.	Fanfold Structure, Conductive Epoxy Applied, Diodes Attached and the Final Devices	34

Figure Page

25. PZT Design for a 2 Channel Gold Plated Device, Nickel Device and a Six Channel Gold Plated Device……..……..……...35

26. Electrochemical Setup for Making the Sharp Pt/Ir Electrodes……..……..……36

27. A Gold Sputtering Machine…...……...……...…38

28. A Step by Step Illustration from PZT Cut Process to Gold Coating with Channels……...39

29. Photographs of the Final PVDF Devices……..……..……40

30. Micro Manipulator Axis…….……43

31. The Force Balance Experiment to Measure the Acoustic Power of the 2.25 MHz……46

32. Photograph of the Electrochemical Setup…….……47

33. Output of a Piezoelectric Element to Ultrasound……...49

34. Short- Pulse Response of a Piezoelectric Element……..……...50

35. Performance of 2mmx 1mm 1layer, 2 Layer, 3 Layer and 3mmx 1mm 1layer, 2 Layer, 3 Layer for a Short- Pulse Setup Across Different Transducers ……..51

36. D33 Vs D31 Measurement in a 3mm X 1mm 2 Layer PVDF Test Material……52

37. Output of a Piezo Electric Element Under Tone Burst Setup……....52

38. Performance of 2mmx 1mm 1layer and 3 Layer and 3mmx 1mm 1layer and 3 Layer for a Tone Burst Setup Across Different Transducers……..……..53

39. Performance of 2mmx 1mm 1layer for a Tone Burst Setup with a 2.25 MHz Transducer Driven by Different Voltages…….....54

40. Performance of 2.5mmx 4mm X 0.305 mm And 5mmx 4mm X 0.305 mm for a Short- Pulse Setup Across Different Transducers…….....……55

41. Performance of 2.5mmx 4mm X 0.305 mm And 5mmx 4mm X 0.305 Mm for a Tone Burst Setup Across Different Transducers……..…….....57

42. Performance of 2.5mm X 4mm X 0.305 mm PZT Device on a Tone Burst Setup with a 2.25 MHz Transducer Driven by Different Voltages……..……..…....58

Figure Page

43. Simultaneous Four Channel Monitoring in a 7mm X 1mm X 5 Layer 4 Channel Series Anodic Device in a Tone Burst Setup ……..61

44. Simultaneous Dual Channel Monitoring in A 7 mm X 5mm X 0.305mm 2 Channel Nickel PZT Device in a Tone Burst Setup……..…..63

45. X Axis Displacement Vs Voltage In Both Channels and Y Axis Displacement Vs Voltage in a 3mm X 1mm 5 Layer Series, 2 Channel Cathodic Stimulation PVDF Device……..64

46. X Axis Displacement Vs Voltage in Both Channels and Y Axis Displacement Vs Voltage In A 7mm X 1mm 5 Layer Series, 2 Channel Cathodic Stimulation PVDF Device…….……65

47. X Axis Displacement Vs Voltage in Both Channels and Y Axis Displacement Vs Voltage in a 7mm X 1mm 5 Layer Parallel, 2 Channel Cathodic Stimulation PVDF Device…….....66

48. X Axis Displacement Vs Voltage in Both Channels and Y Axis Displacement Vs Voltage in Both Channels for a Nickel PZT Device…….....67

49. Voltage Vs Load and Corresponding Current Vs Load Curve Determined from the Voltage Across a Given Load for Nickel PZT Device……..……68

50. X Axis Displacement Vs Voltage in Both Channels and Y Axis Displacement Vs Voltage in Both Channels for a Gold Plated PZT Device……..…….....69

51. Voltage Vs Load and Corresponding Current Vs Load Curve Determined from the Voltage Across a Given Load for Gold Coated PZT Device……..……...70

52. Output Dependence on Conductivity for a PVDF Device……..……71

53. Output Dependence on Conductivity for a Nickel PZT Device…….....71

54. Bode Plot of Impedance Vs Frequency on The Log Scale for a 110um Thick Pt/Ir Electrode Teflon Coated Exposed up to 0.1mm in the Solution for 3 Iterations……..……..72

55. Bode Plot of Impedance Vs Frequency on the Log Scale For A 0.012 Inch Thick Pt/Ir Electrode Exposed up to 5 mm for 3 Iterations……..…….....73

56. Bode Plot of Impedance Vs Frequency on the Log Scale for a 0.02 Inch Thick Pt/Ir Electrode Exposed up to 5 mm for 3 Iterations……...……...73

Figure Page

57. Bode Plot of Impedance Vs Frequency on the Log Scale for a Thin Copper Electrode Coated with Enamel and the Tip Scraped and Exposed up to 3 mm for 3 Iterations…....74

58. Bode Plot Summarizing all the Electrode Plots……74

59. CAP from the Frog Nerve……..…….…77

60. Device Working Output (Gain Of 20 dB) and CAP Results Muffled with Noise……..…...77

61. The Setup on the Left and on the Right the Device was Photographed After Being Placed in the Brain……..……....80

62. A Honeycomb Structure for a 6 Channel Gold Plated PZT Based Device……....85

CHAPTER 1

INTRODUCTION

Neuro-electrical stimulation has tremendous applications in the treatment of neurological disorders and also provide interfaces with the neuro-prosthetics [1]. Some of the neurological treatments include reduction of pain, restoration of lost nerve and muscle function, and relief from a multiple brain disorders like epilepsy, Parkinson's disease and also in cardiac therapeutics.

In most of these applications, stimulation is applied through wired implanted electrodes. This short burst of electrical pulses can suppress epileptic seizures or cause micro stimulation of the brain to restore lost function by evoking a muscle response [2].

Most of these devices are powered by an implanted rechargeable battery with buried wires going in through the skull routed by way of the neck from a lower implanted pulse generator which can cause discomfort to the patient and also makes him/her more vulnerable to infections due to the opening in the skull. This can also restricts their neck movement and patients are often bound to hospitals for longer periods.

There has been reported several wireless methods of charging developed in the recent past as and which also contain an evaluation of these systems [3], [4]. Some of the techniques involved Micro/Radio wave inductive and capacitive coupling to charge the device, which tends to have large losses and interference issues. Optical methods of energy transfer to implants using high intensity lasers [5], has been reported to cause localized heating issues. Acoustic energy transfer methods reported previously by this lab and powered with ultrasound and were found to be effective in creating muscle twitches the sciatic nerve of the rat.

However none of these wireless modalities explored the option of a multichannel device for the above said applications effectively.

The previous said wireless modalities also had devices that were comparatively huge to that required for muscle stimulation. So the need for a compact device and technique to have effective CNS applications is merging.

Ultrasound powered devices have been identified as a good alternative due to the fact that, it is completely safe, and work well within FDA ultrasound exposure limits. Ultrasound is found to

be efficient compared to the other wireless modalities. Also bringing a multichannel perspective reduces the chances of failure of these implants. A doctor can simply put in the device at a target zone and complete the surgery, then wirelessly power them from the outset and if either one of the channels in the target is activated, it can be termed successful.

This thesis evaluated the possibility of multichannel devices constructed out of Polyvinylidene Fluoride (PVDF) plastic and Lead Zirconate Titanate ceramic and powered by ultrasound for the purpose of Intracotrtical microstimulation to provide a novel alternative to the wired multichannel stimulators and also explored the option of multichannel in wireless modalities.

CHAPTER 2

BACKGROUND

2.1 Functional Electrical Stimulation

Electrical stimulation dates back to the Egyptian times, when a patient received strong shocks from an electric eel to produce physiological effects [6]. With the invention of the transistor, it lead to the evolution of implantable pacemakers to tiny injectable devices that can sense and at the same time stimulate the body to restore function in the paralyzed limbs and other parts. They also communicate the signals seamlessly to an external control unit that the user can read.

The first systems to be developed for FES were a 200 multichannel multi wired stimulators that were radio- frequency powered for evoking response in paralyzed arms. This was followed by a 22- channel cochlear implant which was also utilized for leg and other FES applications. Subsequently, FES systems for other applications were also developed, but they were deemed unsuccessful which lead to the beginning of wireless systems.

The problems with the RF powered wired stimulators were

- Extensive surgery was required
- Infections due to large continuous implant surfaces in the body
- Imperfections in placements and antenna problems for powering.
- Long and advanced planning was often required.

Out of the wireless systems, the commercial stimulators that tasted success were the multichannel non-multi wire spinal cord stimulator and the cochlear implant.

These were successful due to the following reasons,

- All the channels were on one or two cables
- Short implantation times
- They were implanted mostly in one or two locations in the body. [6]

2.2 Electrical Stimulation for the Treatment of Epilepsy

Neuro stimulation: When electrical pulses are administered directly on to the nerve or its surroundings, it is found to evoke a physiological response or manipulative to a pathological substrate to achieve therapeutic effect. [7]

Studies show that vagus nerve stimulation by electrical pulses can be a possible cure for the treatment of epileptic seizures. Acute brain stimulation of the thalamic and medial temporal lobe structures has shown positive results in small pilot studies.

The mechanism of action however has been unclear. Multiple hypotheses have been suggested to discuss this action. Some authors have an argument that the efficacy of the process is not in the efficiency of the actual stimulation but rather based on the efficacy of the lesion provoked by the insertion of the stimulation electrode, which is often termed the microthalamotomy effect [8]. Also, it is stated that DBS causes local inhibition induced by the current applied to the nuclei in the particular region that are involved in propagating, sustaining or triggering epileptic seizure activity. Or it may because of the projections spreading from the area of stimulation in an epileptogenic network which includes the medial temporal lobe structures.

2.3 Microelectrode Array for Chronic Deep- Brain Microstimulation for Treating Parkinson's Disease

Electrical stimulation in Deep brain stimulation has been recorded to be an effective treatment modality for treating advanced Parkinson's disease, dystonia and tremors. [9]. However the exact mechanism of action remains unclear yet [10] [11].

A study was conducted using an electrode array that consisted of an assembly which was 16 mm in length and 2 mm in diameter. The electrode array was designed with human trials in mind. The initial studies were conducted on cats in which these electrodes were implanted into the subthalmic nucleus of the brain. The electrodes could stimulate and also record the neuronal activity. These two events however were not simultaneous and were usually one followed by the other.

2.4 Neural Prosthesis

Several external devices were designed to induce spatial temporal patterns of the neural activity. The Neural prostheses generate electrical stimuli that can be used to excite a nerve to initiate action potentials. These potentials can also serve to mimic sensory stimuli thus resulting in evoking muscle responses [12].

Some of the popular interfaces included the cochlear implants. These implants, which are multi- channel interface with the thousands of hair cells and connected to an external processor translate sounds into electrical pulse patterns that can make even restore hearing in a completely deaf individual. Research on Retinal implants have been on the rise, however they haven't been as successful due to the fact that these implants need to address higher density information (from millions of photodetectors on the retina), structure of the sensor and its energy requirements.

Neural prosthesis use the technique of Functional Electrical stimulation reported earlier. This technique has been used in the rehabilitation treatment of spinal cord injuries, increase control of hand grasp and release in quadriplegia, standing and stepping in paraplegia [13] [14] [15] [16], restoration of bladder function, and also treatment of high blood pressure.

2.5 Multielectrode Array for Intrafascicular Recording and Stimulation

Studies have shown the feasibility of implanting an array into the peripheral nerve of the cat sciatic nerve [l]. The Utah electrode array was used for this study, where in the electrodes penetrated the epineurium and reach the intra fascicular region. It has been reported that current injections caused muscle twitches when it was in the range of 10 u. Also, they were able to record compound action potentials that represented selective nerves [17].

This forms the base for the CAP studies which will be undertaken in the later part of this thesis as an animal model to test the efficiency of some of the device.

2.6. Nerve Stimulation: Cathodic and Anodic Stimulation

Nerve stimulation can be of two types. A cathodic stimulation can be provided which is a negative pulse and often the desired kind of stimulation as it is easy to drive the current through the nerve due to the fact that the outside of the nerve is negatively charged.

In Anodic stimulation it is often the opposite case, where the ion channels are broken down to make sure the conduction of current to take place. This requires a lot of current to achieve stimulation.

Hence, the best technique has been to employ Cathodic stimulation for all stimulation needs.

2.7. Current Techniques

The evolution of stimulation techniques have been phenomenal. From wired Utah electrode system array which was used predominantly to record and stimulate the brain to several implants which were powered by wireless techniques like radio waves, Near Infrared laser and Ultrasound.

Below we discuss a few of the modalities.

2.7.1. Wired Modalities

For a functional neuroprosthetic, it required a chronic implantation of microelectrodes for stimulating the nerves and measuring the neve signals. Utah electrode array fell in this category. Several studies were undertaken by several groups [18] [19] [20] [21] for the same application using this system.

It consists of 100’s of miniature electrodes connected to a silicon substrate and is connected to an external battery. This system is then connected to a data acquisition system on the outside for recording purposes. The disadvantages of this modality is the risk of infection and surgical complications, and to accompany that an auto immune reaction can be triggered by the tethering forces associated with the movement of the electrodes. Higher chances of failure of the interconnects due to mechanical stress form the in-vivo settings. Also, this system was found to be more of a discomfort to the patient.

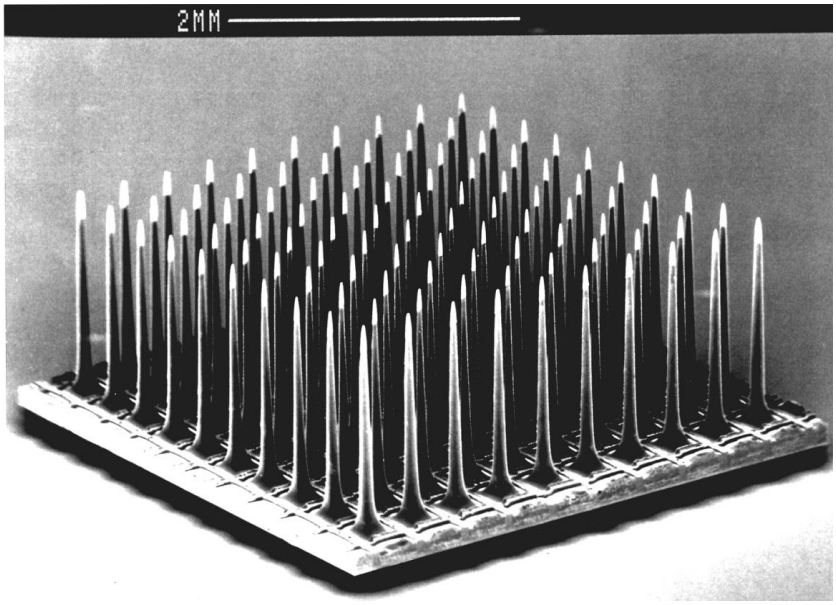


Fig 1: Utah electrode array system
(Source: http://www.sci.utah.edu/~gk/abstracts/bisti03/)

Hence wireless interfaces became the order of the day.

2.7.2. Wireless Modalities

In wireless modalities, energy transfer is often achieved by electro-magnetic, optical, or acoustic methods to the neural tissue to stimulate the neuron remotely or to modulate their activity [2] [22] [23] [24].

Several wireless implantable devices were manufactured and different powering techniques evolved over a period of time. The characteristic sizes of these implantable devices are desired from (10 – 100 μm) as outlined in these studies [3] [25] [26] [27]. Wireless devices bring with them the advantage of reduced infections, high performance, and elimination of the tethering forces mentioned earlier and above all, brings relief and mobility to the patient and not constrained to hospitals.

These devices are powered by different techniques to be discussed below away from the traditional battery powered methods.

2.7.2. (i) Volume Conductive Current

In this technique electrical currents are directly exposed to the tissue, but has been rejected due to concerns over such direct application and problems involved with achieving the required power density at the target tissue region [28]. The energy is applied to the device by high frequency currents conductively supplied to the tissue and relies on transfer through the tissue. Attenuation due to the tissue and also achieving multichannel capability can be a concern, hence this modality was not taken into further consideration.

2.7.2. (ii) Radio or Micro Waves

The radio waves in the frequency (upto 18MHz and sub GHz) were utilized to power the devices using two kinds of techniques

(a) Capacitive Coupling

In this form of powering, which is a pure electric field coupling [29], two parallel plated were placed on either side of the tissue holding the device acted as the dielectric medium. The electrical energy passes through the tissue due to a capacitive linking between the two electric plates. However this technique had limited powering distance, which meant the penetration was smaller.

(b) Inductive Coupling

This technique used the high power coils to charge the device by the method of induction. It is a pure magnetic near field coupling technique. It employed two mutually coupled coils. Radio frequency electromagnetic fields were carried from the source coil to the receiving coil on the device. The frequencies were often limited to below 20 MHz. This powering technique is based on the magnetic component of the wave. For effective powering, it required, huge coils on both the source and receiver which limits its compactness and makes the devices huge. Also this technique is often associated with huge losses due to the distance between the source and the receiver and localized heating of the tissue.

BIONS [23], are a perfect example of inductive coupling and some cochlear implants that used this mode of powering [30].

BIONS did introduce the concept of multichannel. But they were not present on a single substrate. They were individual devices suspended in a tissue that communicate to an external master unit (MCU) and get activated by it. They are often required to be in the range of the MCU but more often their positions are not contained and unknown [6].

2.7.2. (iii) Optical

These kind of devices are powered using the near infrared (NIR) and laser light sources. These systems were termed FLAMES. Semi-conductors were used to convert the light into electrical energy. The reason for choosing NIR is because of the ability to scatter well by the tissue and lesser absorption. Initial studies [31] have shown stimulation of the dorsal pial surface of the rat's spinal cord which elicited a rat upper limb response in the order of 1.08 N. In the later studies [24] the intensities of the light waves were reduced to1.85% of the sub dural after 1mm of the tissue and to about 0.15% at about 2 mm of the tissue depth. The current pulses generated by these devices and employed in the stimulation were around 6 uA to 120 uA. The biggest backdrop of this technique is the localized heating of tissues that can cause discomfort to the patient.

2.7.2. (iv) Acoustic

These kinds of devices are powered using the ultrasound energy in piezoelectric elements which is the main source of study for this thesis. An ultrasound beam travels through a coupling gel and the tissue to reach the piezoelectric element and due to the piezoelectric effect, they cause generation of charges. They have better advantages in terms of better focal spots which means the devices can be made even smaller, higher power densities and lesser attenuation compared to the other modalities.

Several devices employed in several studies [22] [32] [33] [34] utilized this powering modality to elicit nerve stimulation in the peripheral nerves of the rat. Pain relief studies and increasing blood flow to the lower extremities in treating peripheral vascular diseases.

2.8. Ultrasound Properties and Piezoelectric Effect

Ultrasound waves are sound that are of compression and rarefaction properties. These mechanical vibrations are used as an energy transfer technique by way of the piezoelectric effect to generate tiny amounts of electricity.

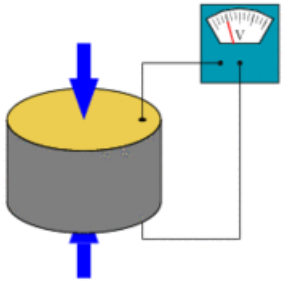


Fig 2: Piezoelectric effect. (Source: https://en.wikipedia.org/wiki/Piezoelectricity)

When force is applied on the yellow phases of the crystal, charge is generated in the crystal.

2.9. General Description of PVDF and PZT and their Interaction with Sound

The PVDF and PZT are piezoelectric materials that have charge generation properties. When electric pulses are applied on two sides of a piezomaterial, mechanical vibrations are seen on the opposite pair of sides as an inverse piezoelectric effect and vice versa. The voltage generated is determined by the pressure (applied force) and the properties of the piezoelectric element [36].

These were the base for devices developed in the last decade [34] [35] [37] [38]. Previous devices from our very own lab created using PZT have been reported to cause motor stimulation in rat [39].

One important theory to be taken into consideration when creating any piezoelectric based devices is the strain coefficients and charge coefficients. They are usually mentioned with a 33, 31 or 15. The piezoelectric element consists of 3 axes and the charge developed depends on which axis the polarization dipole is present and the axis of force [40].

In a 33 subscript, the charge is generated on the same side of the phase that undergoes compression and rarefaction, which means the mechanical stress and the electric field axis are the same that of the polarization axis. In a 31 subscript, the charge with opposite polarity and is generated on the phases which perpendicular to the phase to which the mechanical vibrations are given, which means the pressure is applied along right angles to the polarization axis and the charge though is still generated on the same axis as the polarization. In a 15 subscript, the forces applied is a shear stress and the voltages are generated in perpendicular to the piezoelectric axis.

A g_{ij} constant is the piezo electric constant between the electric field produces to that of the mechanical stress applied [41]. A high g constant is often sought after for implantable device manufacturing.

The polarity of the 33 and 31 values also play a major role. A negative 33 means, when mechanical field is applied, the polarity will be opposite to that of the positive 33 value. The same applies to a 31 as well.

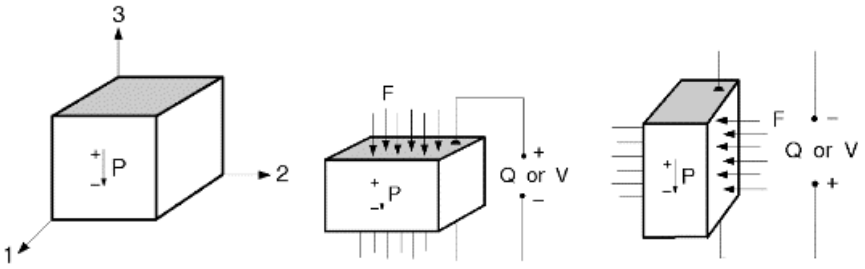


Fig 3: Piezoelectric Axis, 33 configuration and the 31 configuration [42]
Source: Zong, "Applications of Miniaturized Ultrasound Powered Wireless Nerve Stimulators for Pain Management", 2014, 9 – 10.

PVDF – TrFE	d_{33}	-15 (+ or –) 20% pC/N
	d_{31}	6 (+ or –) 20% pC/N
	g_{33}	- 0.186 (+ or –) 20% (V –m/N)
PZT PSI-5A4E	d_{33}	390 x pC/N
	d_{31}	-190 x pC/N
	g_{33}	24 x 10^{-3} V –m/N
	g_{31}	-11.6 x 10^{-3} V –m/N

Table 1: A quick summary on the properties of PZT and PVDF materials used in these experiments

2.10. Single Diode Stimulator Theory

The concept behind the design of the device is from an earlier work already pursued in the ASU laboratory. It has been established that a piezoelectric element with a diode in parallel and electrodes attached produced a DC rectified output that is neurostimulatory [43].

As mentioned in the literature, devices for microstimulation applications in the Central nervous system need to be really small and the components of it limited. Any additional component that can increase the size of the device needs to be avoided because of concerns related to tissue trauma in bigger devices [24].

2.11. Conductivity of Different Tissues

The conductivity of the tissue plays a major role in the electrical load presented to electrodes, in other terms the conductivity of the tissues are desired to be known so to manufacture the devices whose output impedances match that of the electrode- tissue impedance for effective power transfer. The following values were sourced from a well-known scientific literature website [44].

ALL TISSUES, SINGLE FREQUENCY

FREQUENCY = 1000 Hz

Tissue name	Frequency [Hz]	Conductivity [S/m]	Relative permittivity	Loss tangent	Wavelength [m]	Penetration depth [m]
BrainGreyMatter	1000	0.098805	164060	10.826	303.79	53.022
BrainWhiteMatter	1000	0.062574	69811	16.112	387.55	65.628
Cerebellum	1000	0.1188	164360	12.993	279.18	47.984
CerebroSpinalFluid	1000	2	109	329830	70.71	11.254
Nerve	1000	0.028774	69911	7.3982	551.11	100.36

FREQUENCY = 1000000 Hz

Tissue name	Frequency [Hz]	Conductivity [S/m]	Relative permittivity	Loss tangent	Wavelength [m]	Penetration depth [m]
BrainGreyMatter	1000000	0.16329	860.42	3.4114	6.7724	1.4392
BrainWhiteMatter	1000000	0.10214	479.79	3.8266	8.6953	1.792
Cerebellum	1000000	0.1854	1140.8	2.9213	6.2085	1.3826
CerebroSpinalFluid	1000000	2	108.99	329.85	2.2326	0.35642
Nerve	1000000	0.13026	926.14	2.5283	7.2243	1.6912

Table 2: Conductivity of different tissues at the two different frequencies

CHAPTER 3

METHODS

3.1 Construction of the Neurostimulators

In this work two kinds of devices were explored to carry out a comparative study.

1) Polyvinylidene fluoride, commonly abbreviated as PVDF and
2) Lead Zirconate Titanate, also known as PZT.

These were the piezo electric materials used. Both the neural stimulators follow a simple generic design as shown in the figure below that follows the Single Diode Stimulator theory [43] discussed earlier.

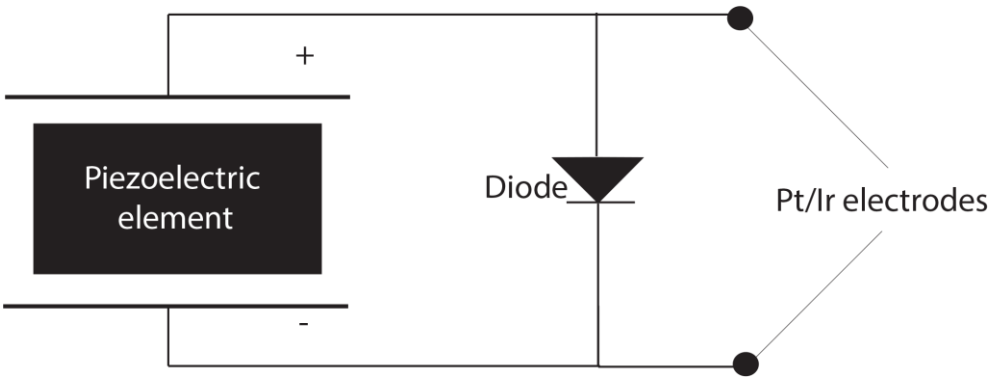


Fig 4. Single Diode Stimulator design

The central piezoelectric element has a diode that is in connected in parallel using silver epoxy and the device is concealed in a biocompatible polyimide tubing concealed with hermetic nonconductive epoxy.

Some of the design requirement goals that were considered in the final design

1) Small and compact design: Smaller than 8mm for effective CNS applications
2) Multichannel capability
3) Matching output port impedances to that of the tissue where the device is to be implanted, so as to have maximum efficiency

3.2 Characterization Study of the Piezoelectric Materials

The two piezomaterials were first characterized for its output performance i.e. the maximum AC voltage produced. Several test specimens were constructed to test performance in conditions ranging from no load to different loads. This study was essential in understanding the material better in creating the design to meet the requirements of neural stimulation.

The study evaluated PVDF and PZT on the following 3 factors:

- Length
- Thickness

  Vs powered by different frequency transducers and different voltages to finalize on an ideal piezoelectric material.

3.2.1. Design of PVDF Test Material for Characterization

To make the test specimens, PVDF sheet of 220um thickness sourced from KTech Corp was considered.

The following dimensions and thickness were considered for this study

- 2mm X 1mm X 220um
- 2mm X 1mm X 440um
- 2mm X 1mm X 660um
- 3mm X 1mm X 220um
- 3mm X 1mm X 440um
- 3mm X 1mm X 660um

The PVDF was carefully measured using a Vernier caliper for the different lengths and they were cut using a micro surgery scissors under a compound microscope. Additional care was taken in handling the PVDF by always wearing a surgical glove so as to remove the possibility of stray static charges from the body getting onto the material.

Once the material was cut, they were marked for its polarity to make sure the connections were made right

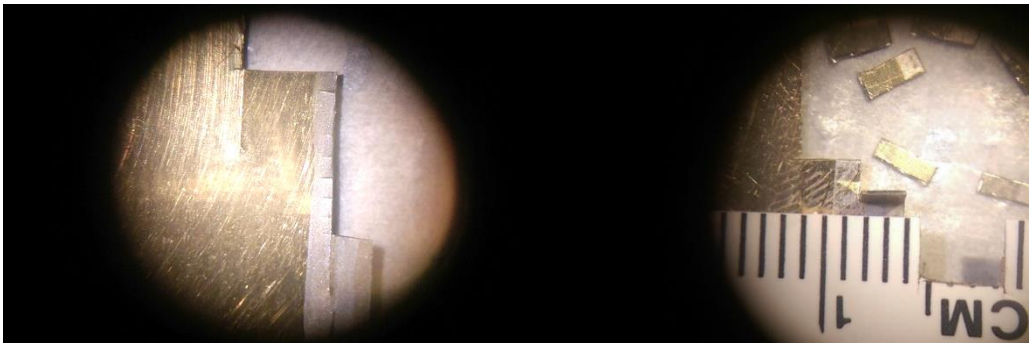


Fig 5: An example of the PVDF sheet with the positive polarity marked and cut

To achieve the different thicknesses, several layers of PVDF were serially attached one above the other to make a stack using conductive epoxy from MG Chemicals shown in the figure below.



Fig 6: MG Chemicals Conductive epoxy

The epoxy consists of two parts: Part A and Part B which have a pot life of 10 minutes and 5 minutes respectively.

These epoxies were mixed in a ratio of 1:1 by weight on a micro weighing scale and left to sit for about 10 minutes. This reduces the viscosity of the mixture and gives a more solid sticky nature that is ideal to stick the PVDF materials as it reduces the chance of runoff of the liquid and potential shorting of the two conductive layers of the PVDF.

Selective quantities of the epoxy were applied using a thin wire and the layers were sandwiched.

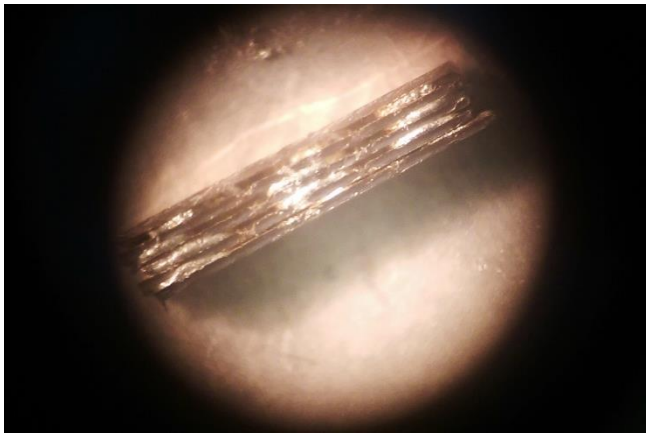


Fig 7: Sandwiched PVDF layers. The negative poled side of one layer is attached to the positive side of the next sheet to form a series interconnect

The epoxy has a curing time of about 24 hours under normal room temperature at 25 ^{o}C. The sandwiched layers were allowed to cure for a day with additional heat lamps placed to enhance the cure. These heat lamps heat maintain a temperature of 35^{o}C at the surface of the aluminum slab that hosts the devices.



Fig 8: Heat lamp setup to cure the PVDF Layers.

Once the layers are cured, they were tested in the experimental setup, which will be discussed shortly.

3.2.2. Design of PZT Test Material for Characterization

For the design of test materials, elements sourced from Piezo Systems Inc were used. The following dimensions were considered.

- PZT- 5A (Thickness - 0.0050”)
    - 2.5mm X 4mm
    - 5 mm X 4mm
- PZT- 5A (Thickness - 0.0075”)
    - 2.4mm X 4mm
    - 5 mm X 4mm
- PZT- 5A (Thickness - 0.0120”)
    - 2.5mm X 4mm
    - 5 mm X 4mm

Cutting the Piezoelectric ceramics:

The PZT ceramics were cut using Universal Laser Systems – 40 W CO_2 based laser



Fig 9: Universal Laser Systems(ULS) 40 W Laser systems (Source: http://www.ulsinc.com/products/)

The designs were created using Adobe Illustrator

The test materials were designed with respect to the final design in mind. The holes were provided for the soldering of the diodes in the final device.

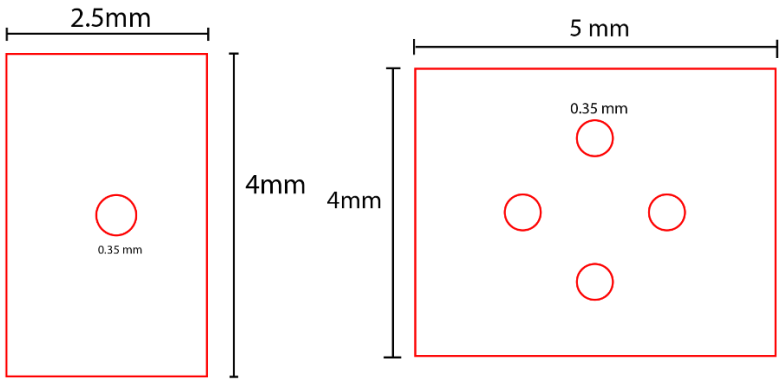


Fig 10: PZT Test materials

Additional care was taken to make sure the PZT cuts are made precisely. The PZT was handled with gloves and tweezers and placed on an aluminum sheet and taped for providing additional mechanical support and also to prevent the cut devices from falling off into the honeycomb pored base of the laser system. The aluminum sheet and the PZT is wiped with alcohol swabs to remove dust and possible finger prints. The CO_2 laser heats the PZT material and makes the cut. Usually the process was repeated 7 – 8 times with the adjustments in power and speed increased gradually. Too many repetitions were also sometimes avoided, so as to make sure the Nickel coating on the PZT isn't removed due to the excessive heat of the laser and also making the ceramic brittle. The material was assessed after each print, while still in place on the laser base and a reprint was done only if necessary. Once the print process was done, the material was removed and the cut PZT's were extracted using a tweezer. About 10 cm of enamel coated wires with the end insulation scraped off using a grinder were then soldered onto the each side of the PZT so as to connect the measuring probes during test experiments.

The below figures give a brief overview of the design process to cut.

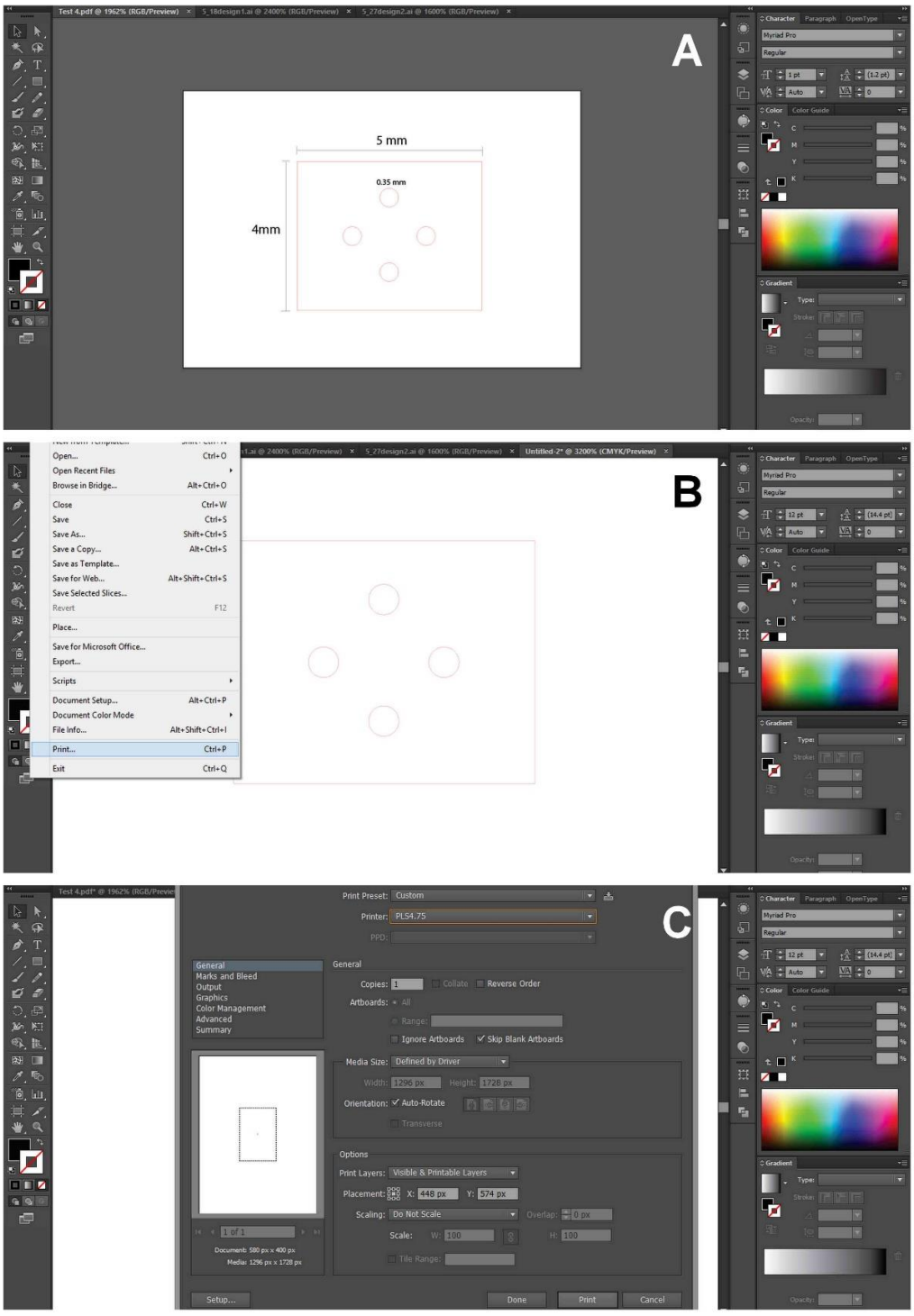


Fig 11: Pictorial representation of the design process to print in Adobe Illustrator A: The design was created. B: The design was then printed by choosing "Print" from the "File" Menu C: The printer "PLS 4.75" is chosen and then choose "Print"

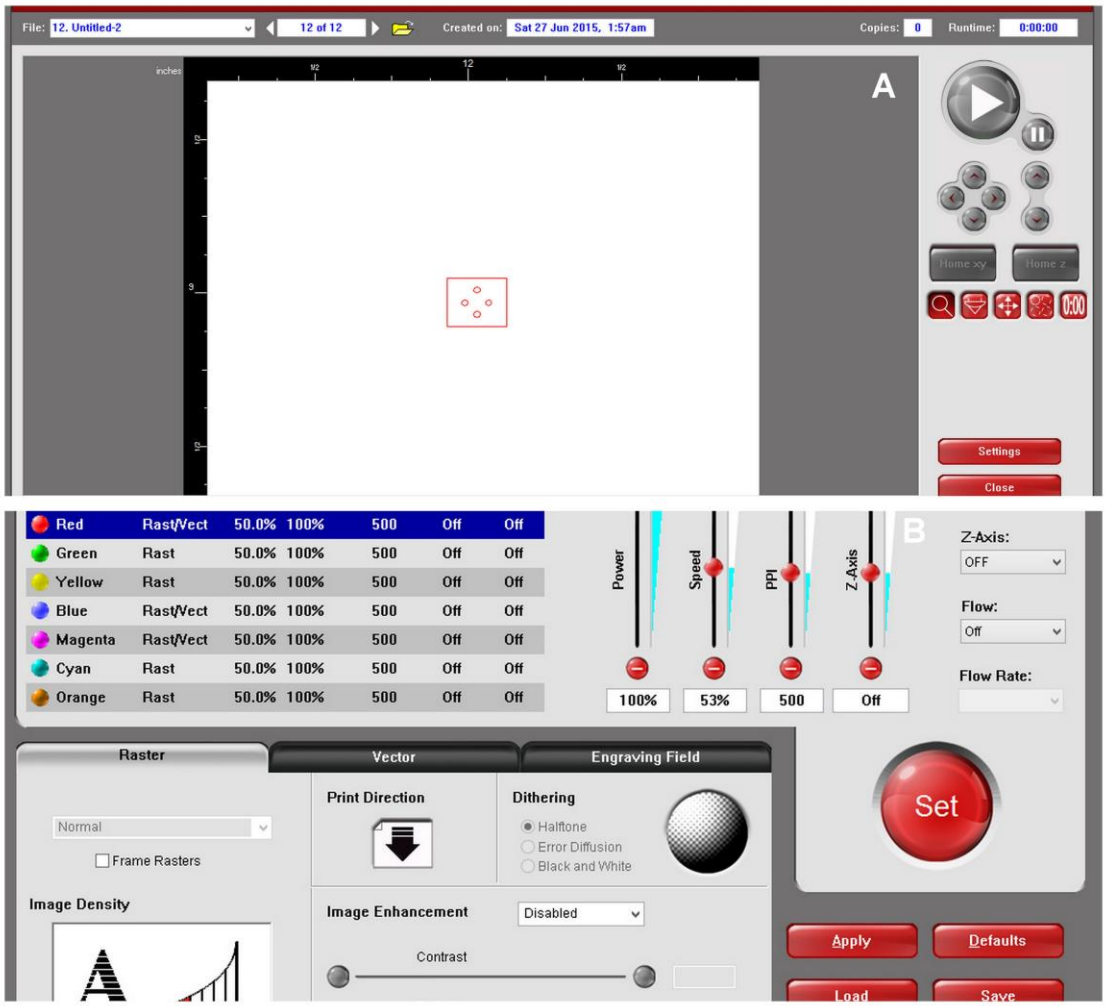


Fig 12: ULS Print interface.
A: The design in the main dialog box. B: Settings menu: Adjusting the Power and Speed of the cut for each color to arrive at the required cuts.

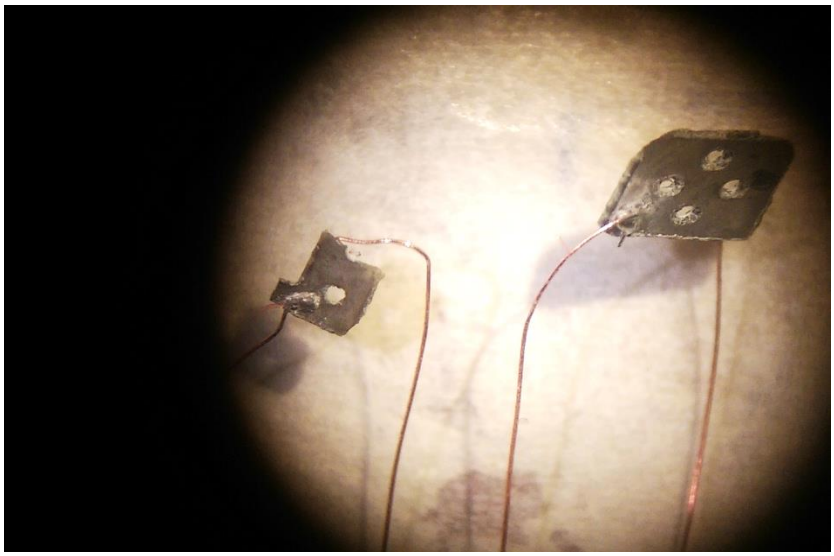


Fig 13: The test devices after the laser cut process. One can note the improper edges due to the fragility of the ceramic, if the process isn't done correctly.

The devices are now ready to be tested in the experimental setup. It must be noted at this point that only the 0.012" PZT ceramic was mechanically stable at the end of the laser cut procedure and were considered for further study and for making the final devices.

3.3. Experimental Setup

The aim of this study was to observe the performance of the different test materials with respect to different frequencies of ultrasound pulses.

- 2.25 MHz
- 5 MHz
- 20 MHz

Two different setups were considered

Setup 1- Short pulse response system: This setup also referred to as Panametrics setup has an Ultrasonic Pulser- Receiver system from Panametrics Inc. that generates 100 V single pulses with 100uJ energy. The advantage of this system is that, the output is read as an echo and has an inbuilt amplifier that can provide up to 60 dB gain. And for our experiment a gain of 20dB was chosen.

This system is used with the 2.25, 5 and 20 MHz transducers. The experimental setup is visualized in the block diagram below.

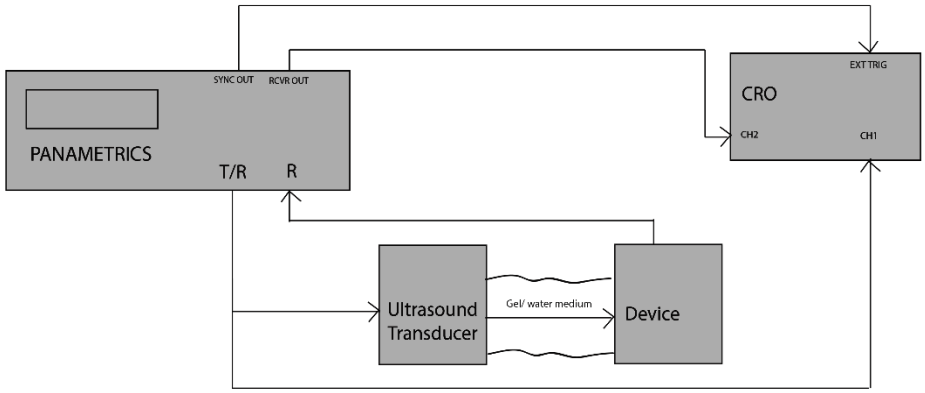


Fig 14: Setup I Block Diagram Panametrics Inc Ultrasonic Pulser – Receiver system

A splitter was added to the Transmitter socket (T/R) and one probe was connected to the transducer which was coupled with the device either by immersing it in a water bath (which has a stage that holds the device to keep it from changing direction during the experiment) or by attaching a cut syringe structure with distilled water and gel suspended perpendicularly on top of the transducer as shown in the figure below.

The PVDF test devices are usually held using a tweezer (which has a capacitance of about 7pf) which in turn has wire tips to connect to a measuring probe, whose overall capacitance was around 155 nF. The PZT devices were held using a clay stage inside a water bath or suspended in gel with measuring electrodes suspended outside of the gel.

The other probe from the transducer socket was connected to Channel 1 of the CRO to measure the input signal going to the ultrasound transducer.

The measuring probe was connected to the device or the tweezer and connected to the receiver socket (R) on the Short- Pulse pulser/receiver. A cable from the “SYNC OUT” is connected to the external trigger of the CRO to trigger the signals based on the Input pulse.

A probe is connected from the receiver out (RCVR OUT) to the CRO where the output signal was measured.

Setup 2- Tone Burst response system: This setup also referred to as the Ophir setup has a signal generator system which is gated by a pulse generator which is in turn connected to a Linear Power amplifier. The signal generator generated a signal that is in resonance with the transducer frequency. The Pulse generator's gate signal determines the pulse duration and the repetition rate. The intensity of the signal is adjusted by the voltage that is applied to the transducer which is in turn controlled by the voltage applied to the Linear Power amplifier.

For the purpose of this bench test, with a 2.25 MHz transducer the input signal was a 2.25 MHz signal modulated with a 25us wide pulse from the pulse generator with a 50ms interval.
The reason for this approach, which is considerably more complex, was to avoid transmit burst artifacts from interfering with the signal evoked from the nearby piezoelectric through capacitive coupling. The use of transit time delay cleanly separates the piezoelectric signal from the interference of the ultrasound transmitter. This system was tested with a 2.25 and 5 MHz transducer.

The experimental setup is visualized in the block diagram below.

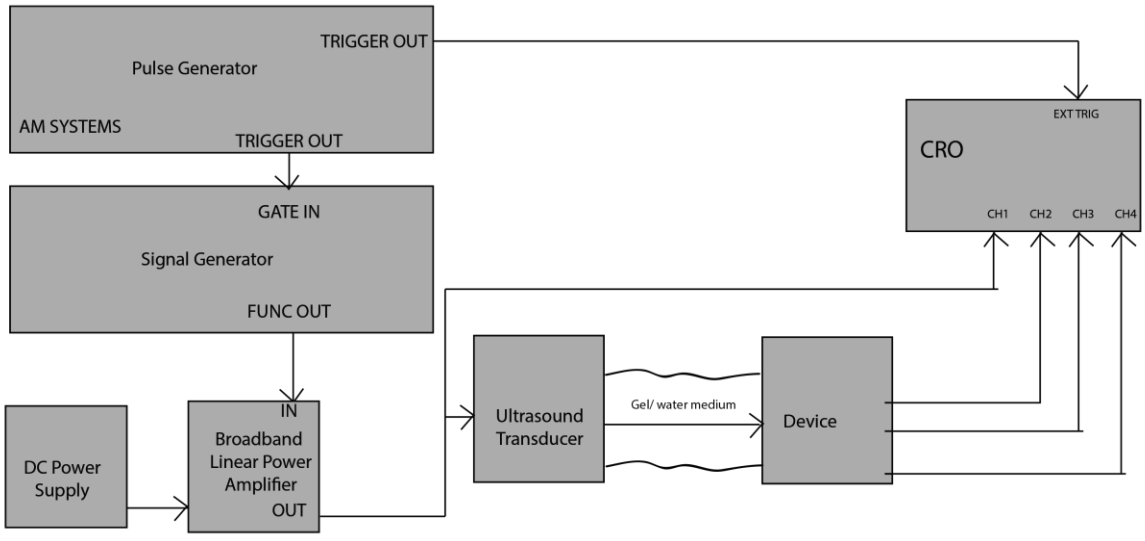


Fig 15: Setup II: Tone burst response system.

The goal of this instrumentation setup is to create a selectable ultrasound burst duration and repetition rate using a combination of equipment that employed modulation of a CW signal generator having an external modulation capability.

Also, the actual setup is photographed as shown in the figure below.

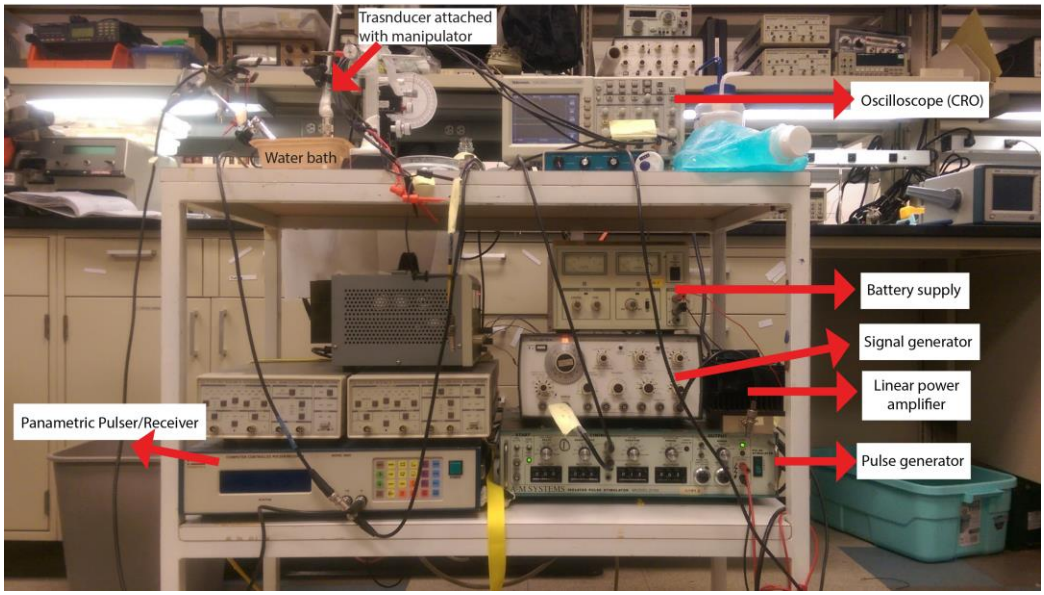


Fig 16: Overall assembly of the setup on a movable table.

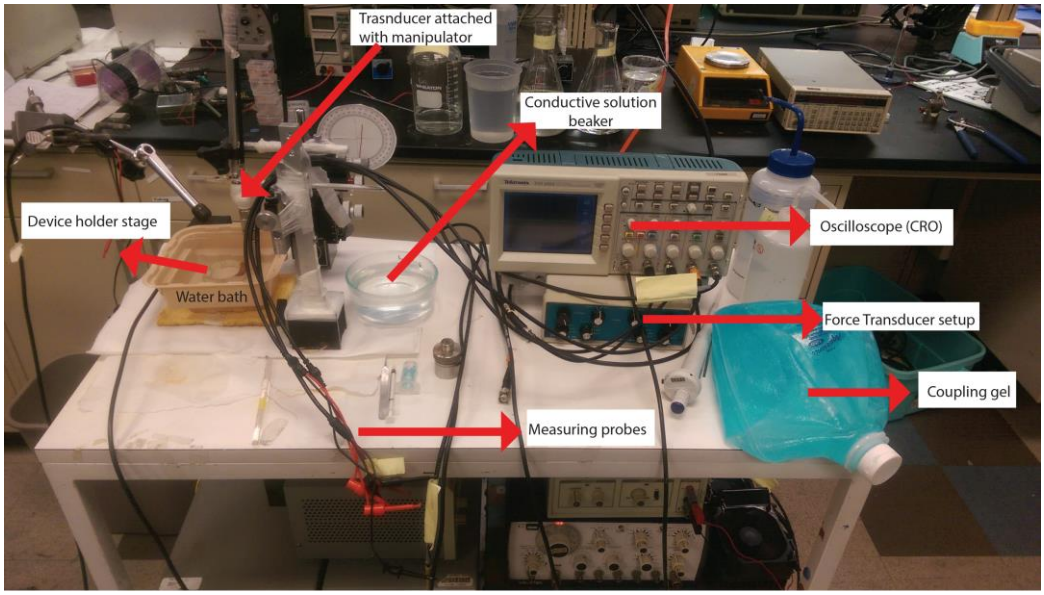


Fig 17: Top view with the water bath setup. The device is suspended in the water bath on a stage and the transducer attached to a manipulator is suspended in the water and moves in the 3 axis X,Y,Z

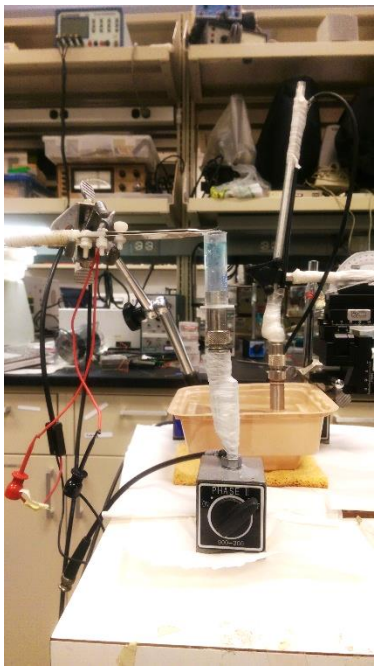


Fig 18: A tweezer setup with the Ultrasound transducer suspended perpendicularly upwards with a syringe cup (different cups measuring the size of the focal length of the beam of the respective transducers, is filled with water and non-conductive gel)

3.4. Experimental Procedure

Setup 1:- Short – Pulse response system.

Step 1: The test devices were held in the tweezers or suspended in the gel medium which has negligible conductivity.

Step 2: The transducer was powered by the Pulser/Receiver.

Step 3: A load setup (a set of resistors connected to a bread board) was connected in parallel to the device.

Step 4: The measuring electrodes read the output of the device vs different loads.

Different transducers (2.25, 5, 20 MHz) were attached to the system and the corresponding readings from the device were noted.

For the PVDF devices, they were held in place using the tweezer which also acts as contacts for the PZT. They hold the PZT suspended in the gel at the very edge so that maximum surface is exposed to the ultrasound beam.

The tweezer was moved around to make sure the devices fall in the range of the ultrasound beam, so that the full beam was focused on to the devices.

An additional D33 vs D31 measurement was also recorded for a 3mm X 2 mm 2 channel device to compare the output generated between the two.

Setup 2:- Tone burst response system

Step 1: The test devices were held in the tweezers or suspended in the gel medium which has negligible conductivity.

Step 2: The transducer was powered by the Linear Power amplifier.

Step 3: A load setup (a set of resistors connected to a bread board) was connected in parallel to the device.

Step 4: The measuring electrodes read the output of the device vs different loads.

Different transducers (2.25, 5 MHz) were attached to the system and the corresponding readings from the device were noted.

The same procedure was followed with respect to Setup I in terms of holding the devices.

An additional test was performed on 2mm X 1 mm 1 layer PVDF device and also the 2.5mm X 4 mm PZT device with a 2.25 MHz transducer with different driving voltages to understand the performance of the device vs different driving voltages on the transducer.

The results from these experiments were compiled in the results section which will be discussed there.

The above work employed two different types of ultrasound characterization systems. The reason was the inability to detect a significant signal from the devices at high frequencies using the simple pulse-response system. The tone burst system gave a much higher signal to noise ratio in general although was far more complicated to construct and get to work properly. The short pulse-response system of the Short- Pulse Inc. tester was used as an initial study so to choose the combination of materials and dimensions to make the actual devices for further bench test study.

Working with PVDF material increased the manufacturing times, as all the epoxy had to set at room temperature. Any temperature rise beyond 85 ^{o}C meant the depolarization of the PVDF

material. Several dimensions of PVDF were cut to perform the bench study and the layers were serially connect to test their output performance.

The output that was read across the devices in both the setups was comparatively lesser than what would have been the theoretical output. This is due to the parasitic capacitance of the tweezer combined with the capacitance of the overall setup on the recording end and the probes that leads to a value lesser than the actual output.

At the end of these experiments it was established that by increasing the number of layers one can expect an increased output, subjected to the transducer used and also the area didn't play a significant role, rather the number of layers determined the voltage. In some cases a higher frequency transducer generated lesser output in the devices and hence after a thorough deliberation, 2.25 MHz was chosen as the best transducer to power the PVDF devices.

The characterization of PZT was done with test materials constructed similar to what would be the final devices. Using state of the art 40 W universal laser systems precise cuts were made. The process was iterated over multiple times and it was a progressive increase between each iteration to make sure the end result was as expected, a more sturdy material as opposed to a brittle material. Deliberate spaces were made for what would be the diodes placed and most of the bench tests were performed.

After all the characterization experiment results were studied, it was established that 2.25 MHz transducer was the ideal transducer to be used, as it was a focused transducer with a higher penetrable depth than the 5 MHz and above frequency transducers. Also it has a higher wavelength than the 5 MHz frequency transducer as the wavelength is inversely proportional to frequency.

3.5. Capacitance Measurements of the PVDF and PZT Test Devices

The capacitance of the different devices were also measured using a digital capacitance meter.

The results of which is compiled in table 4 and table 5.

This is necessary to draw a comparison between the recorded value and the actual value and the output can then be projected so that the recorded values can scaled to the actual values.

Based on a comparative analysis of the results from the above characterization tests, insight was gained in how the output changed in series versus parallel combination. This information was used in the subsequent design of the devices finally tested.

3.6. Fabrication of PVDF Based Neurostimulators

Several PVDF devices were built to be bench tested and employed in animal studies. A comprehensive list of the devices made is as follows.

PVDF	Type of Stimulation					
Type of layer interconnect	Anodic Stimulation			Cathodic Stimulation		
Series Interconnects	Dimensions (mm X mm)	Layers	Channels	Dimensions (mm X mm)	Layers	Channels
	3 X 1	5	1, 2	3 X 1	3	2
	7 X 1	5	1,2,3,4	3 X 1	5	2
Parallel Interconnects	3 X 1	5	1	-	-	-
	7 X 1	5	1,2	-	-	-

Table 3: PVDF device dimensions

Both single channel and multi channels were constructed. In the multichannel devices cathodic as well as anodic devices were made. Cathodic devices have distinct individual electrodes coming out of the negative side of the piezoelectric element and the ground or the return electrode is a common positive side of the element. In anodic devices it's the opposite, they contain distinct positive electrodes and a common negative or the return electrode.

The several layers of the PVDF were either serially connected as done with the test devices or were parallel connected using a fanfold like structure, as shown in the figure below.



Fig 19: A fanfold structure with an even number of folds, so that the positive side of the pole ends up on the top and the bottom end of the fold is negative

This was done so as to increase the capacitance of the base piezoelectric material so that the output port impedance matched that of the tissue. The serial devices had a very high output port impedance due to their very low capacitance which were calculated by first measuring the capacitances and then the impedances practically measured and also theoretically calculated and verified.

3.6.1. (i) Construction of Anodic Stimulation Devices – Series Interconnects

An anodic stimulation device was constructed using a PVDF stack up to 5 layers with a diode in parallel connected using silver conductive epoxy with Platinum iridium (PT/IR) electrodes and enclosed in a biocompatible polyimide tube and sealed with Biocompatible non-conductive epoxy.

3mm X 1mm & 7mm X 1mm 1 channel – The stack was made using 5 layers of 220um PVDF sheet sourced from Ktech.Corp cut to the appropriate dimension. The layers were marked and cut using a Vernier calipers and micro surgery scissors. Silver conductive epoxy already discussed in section 3.2 in the test device fabrication is used again to make the interconnects.

A Schottky diode SMS 7630- 079 LF package from Skyworks solutions inc. which has a bias voltage of 150 mV was attached in parallel to the PVDF stack. PT/IR (90% PT, 10% IR) about 0.010” thickness and about 5mm was cut and attached to the positive and the negative sides of the stack. A non-conductive epoxy was prepared by mixing Part A and Part B of 303-3M from Epoxy technology in the ratio 100:45. The device was then introduced into a polyimide tube and filled with the non-conductive epoxy carefully without any air bubbles. The device was then left to settle on an aluminum slab at room temperature (about 23 ^{o}C) for 24 hours with a heat lamp projecting a heat of 35 ^{o}C to the surface of the device

3mm X 1mm 2 Channel, 7mm X 1mm 2, 3 & 4 Channel Devices

For a 3mm X 1mm 2 channel device, special care was take in preparing the stacks. A single sheet layer is taken at a time and the gold/platinum coating around 0.2 mm X 1mm on both sides was carefully removed by scratching using a micro scissor. So effectively there are 2 channels with 1.4 mm X 1mm of gold coating on either side of the junction. The steps are repeated for all the 5 layers. Silver epoxy was carefully added onto both sides of the junction carefully and the layers are sandwiched. Two diodes from Skyworks as from the 1 channel device are added in parallel for the 2 channels and the metal electrodes were attached. The device was then introduced into polyimide tubing and sealed using a non-conductive epoxy. The process was photographed and presented below in Figure 21.

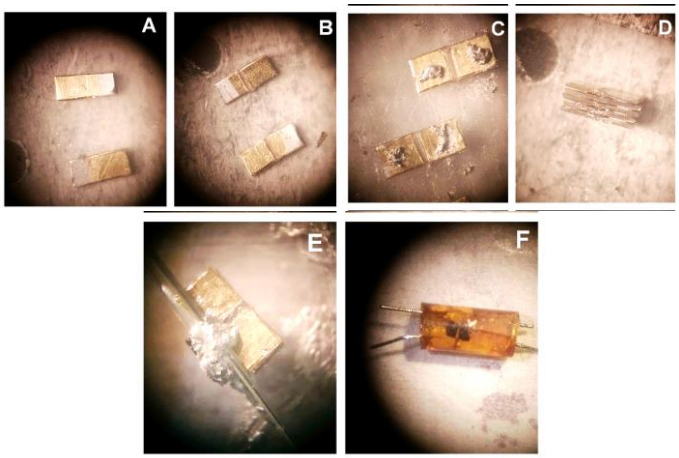


Fig 20: Step by step illustration of the whole process, A: The layers are cut, B: The metal layer is scraped, C: The conductive epoxy is carefully placed on both the layers, D: The layers are sandwiched, E: The diodes and the electrodes are attached, F: It is enclosed in the polyimide tube with Non – Conductive epoxy.

For a 7mm X 1mm 2, 3 and 4 channel the same procedure was followed. The only difference being the way the layers were created. For a 2 channel, 0.2mm X 1mm metal coating was removed on both sides of the 220 um layer for all the 5 layers so there is an effective 3.4 mm X 1 mm of gold on both sides of the junction. For a 3 channel, 0.2 mm X 1 mm is removed at two spots as shown in the fig and for a 4 channel device a center vertical section of metal of about 0.2 mm X 1 mm was scraped and a horizontal section of 3.4 X 0.1 mm was removed on both sides to create a grid as shown in the fig 22.

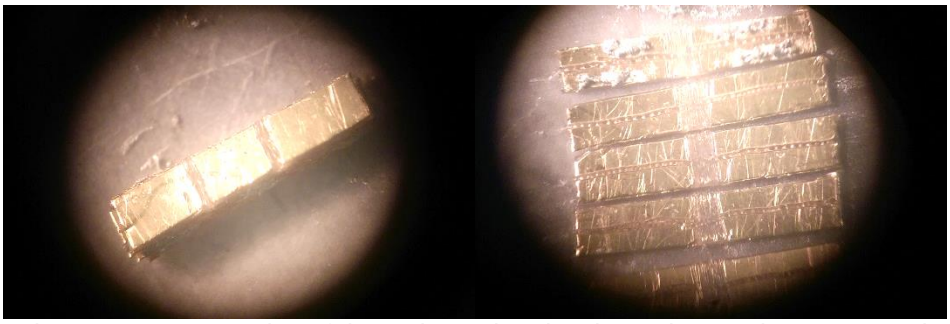


Fig 21: A representation of the 3 channel and 4 channel PVDF layers created.

The rest of the steps follow that of the earlier devices made. The electrodes length varied for the 3 channel and 4 channel devices. Find below a picture of the 3mm X 1mm single and dual channel and 7mm X 1mm 3 channel device in their final packages pictured.

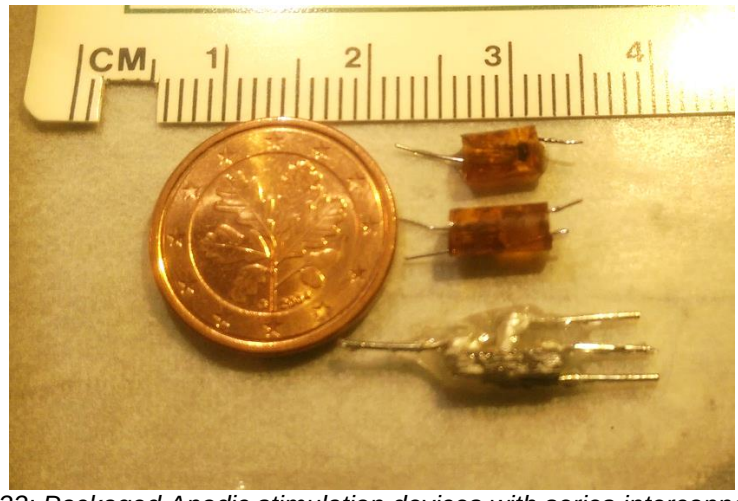


Fig 22: Packaged Anodic stimulation devices with series interconnects.

3.6.1. (ii) Construction of Cathodic Stimulation Devices – Series Interconnects

Two devices were constructed. 3mm X 1mm 3 layer and 5 layer devices. The same procedure was followed as that of the anodic devices. The only change being, a 0.005" PT/IR (90%:10%) was attached. The negative electrodes were distinct and the common return electrode was the positive side. Find below a photograph of the devices

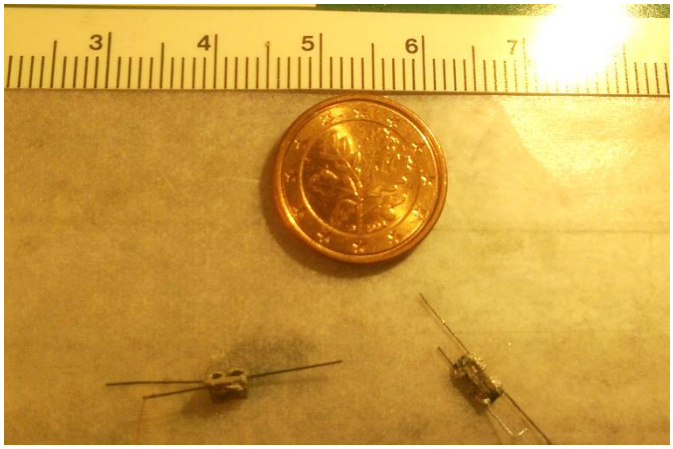


Fig 23: On the left a 3mm X 1mm 3 layer device and onto the right a 5 layer device.

3.6.1. (iii) Construction of Anodic Stimulation Devices – Parallel Interconnects

An anodic stimulation device was constructed using a PVDF stack up to 5 layers with a diode in parallel connected using silver conductive epoxy with Platinum iridium (PT/IR) electrodes and enclosed in a biocompatible polyimide tube and sealed with Biocompatible non-conductive epoxy.

3mm X 1mm and 7mm X 1mm 5 Layer Devices Single Channel:

The parallel interconnects were made by folding the 220 um sheet into a fan fold kind of structure.

For a 3mm X 1mm device, about 20 mm X 1mm of long PVDF sheet was cut and folded at every 3 mm to achieve a parallel layered stack. For a 7 mm X 1mm device, 40 mm X 1mm long sheet was cut and folded. Conductive epoxy was added in between the layers and taped to hold the layers in place. These were left to set for a day and the diodes and electrodes 5mm long (PT/IR

90%:10% 0.0012”) were attached the following day and again left to set on an aluminum slab for a day at room temperature with a focus light that projects a surface temperature of about 35 ^{o}C.

For these types of devices, non-conductive epoxy as mentioned earlier was then added with the device suspended at a height from the slab so that it spreads all over the device and was left to set for an additional day with the similar settings mentioned before.

7mm X 1mm 5 Layer Devices – 2 Channel

For a 2 channel device two 3mm X 1 mm parallel devices were placed on a common conductive platform with both the negative sides connected with conductive epoxy and the whole device sealed in the Non-conductive epoxy.

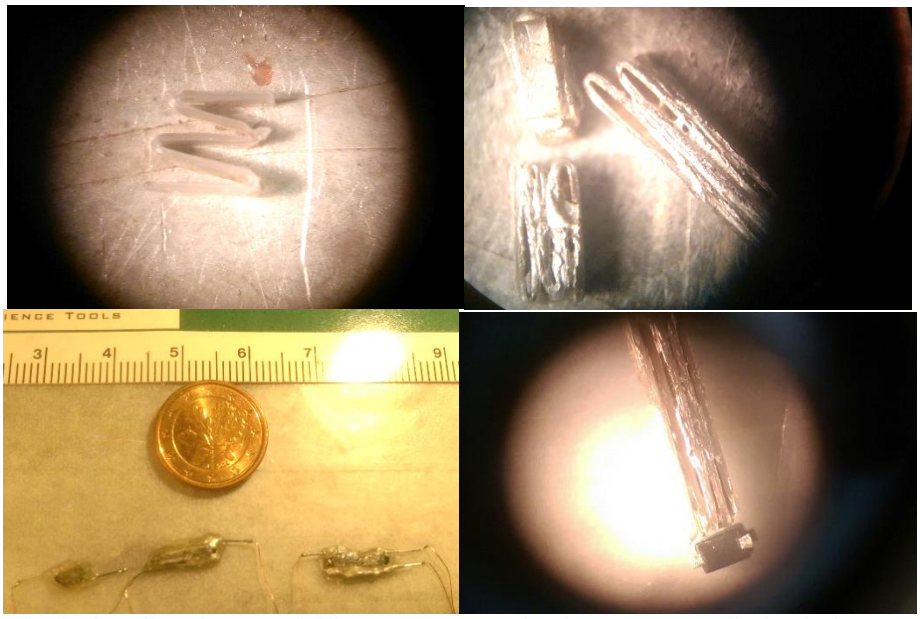


Fig 24: In clockwise direction: Fanfold structure, Conductive epoxy applied, Diodes attached and the final devices

3.7. Capacitance Calculations of PVDF Neurostimulators

The capacitance of all the base materials of PVDF devices were measured using a capacitance meter to calculate the output port impedances. As each of the piezoelectric layer is nothing but a PVDF with two metal layers, it is seen as similar to that of a capacitor. So the formula for the capacitive reactance is used.

$$X_C = \frac{1}{\omega C} = \frac{1}{2\pi f C}$$

Where Xc = Capacitive reactance

F= frequency of the input pulse

C = Capacitance of the base material

3.8. Fabrication of PZT Based Neurostimulators

The fabrication of the PZT device requires additional procedures compared to the PVDF manufacturing.

A PZT- 5A of thickness 0.012" was chosen. The following designs were conceived as interesting and compact ways to achieve multiple channels and then laser cut out of the PZT. The cutting procedure is similar to that mentioned in the section 3.2.2.

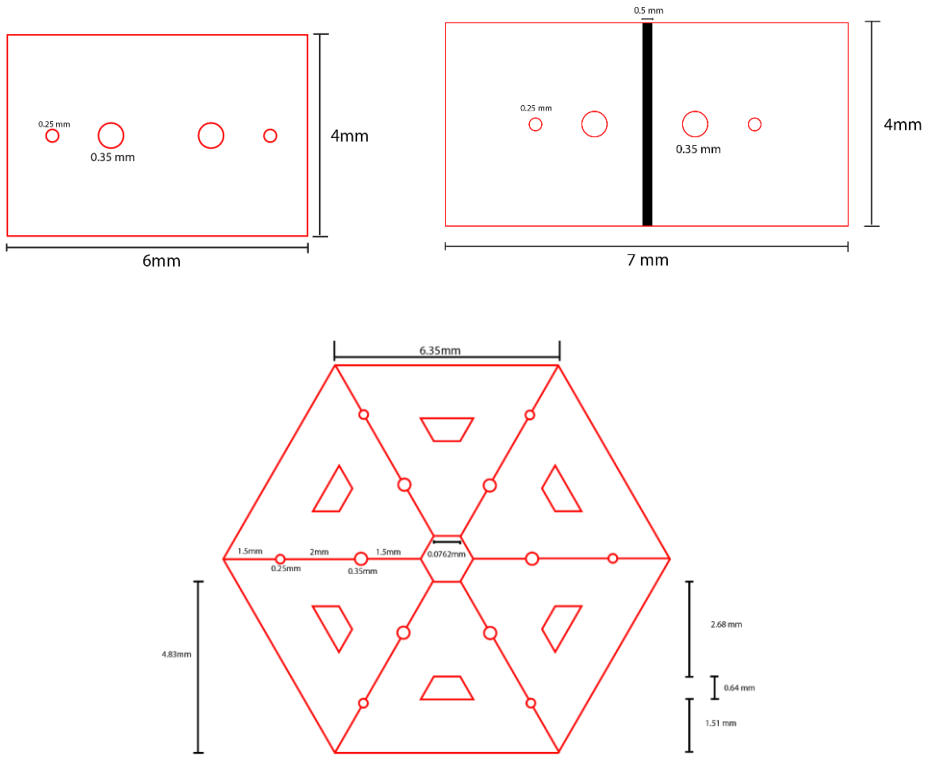


Fig 25: Clockwise from top, PZT design for a 2 channel gold plated device, nickel device and bottom is the 6 channel gold plated device.

It has to be noted at this point that in the second design for the nickel device a black line was drawn and the laser settings was adjusted to make sure that the laser strategically removed just the nickel layer on top rather than creating a cut thereby creating the distinct channels required. For gold coated devices a different procedure is followed for making the channels to be discussed in the following sections.

Electrode Preparation

Before the discussion on the manufacturing of the gold and nickel devices is initiated, the procedure to make the specialized electrodes to attach to the devices is mentioned.

For the purpose of brain stimulation, sharp and insulated electrodes are required so as to penetrate the brain and reach the 5th layer, which is the motor cortex.

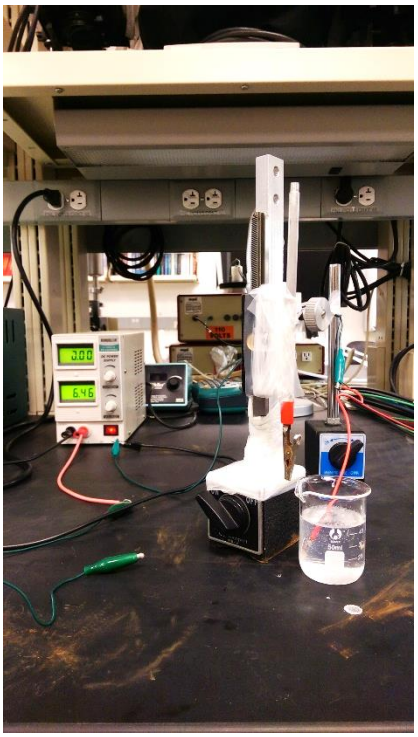


Fig 26: Electrochemical setup for making the sharp PT/IR electrodes

An electrochemical etching setup was designed. A saturated potassium chloride KCL solution was prepared by continuously diluting the salt in 500 ml of deionized water in a beaker with a magnetic stirrer and heated to 50 ^{o}C. About 10 ml of this solution is taken in a 20 ml beaker.

A Copper plate of about 5mm X 5 mm was cut and a wire was soldered onto it which acts as the cathode and is connected to the negative port of the DC supply. The PT/IR electrode (0.010”) with Teflon coating was attached to a micromanipulator with about 0.1mm of Teflon coating removed at the tip to facilitate more etch. This electrode was connected to the positive supply of the DC power source. Both the anode and the cathode was dipped into the electrolyte solution and a DC voltage of about 10 V was applied. The micromanipulator was slowly moved upwards to achieve a sharp etch similar to that of a needle. Once the process was completed about 5 mm of the electrode from the tip was cut to make the electrode and the process was repeated to make sufficient electrodes to be attached to the devices.

3.8.1. Gold Coated Devices

The gold coated device needs additional preparation in making the channels.

Required chemical reagents were prepared as follows

10 % Nitric acid solution: This was prepared from a 63% nitric acid solution by diluting 158.73 ml of the acid to 1000 ml by adding deionized water.

20% by mass KOH solution: This was prepared by diluting 20 gms of Potassium hydroxide in 100 ml of deionized water.

Making of the channels on the PZT, The step by step procedure is as follows:

1. The PZT material is first placed in the nitric acid solution for about 20 minutes. The nitric acid completely removes the nickel coating on both sides. The PZT is removed and cleaned in deionized water and left to dry.
2. A microposit photoresist is then applied marking the channels on the negative side of the PZT and is baked in the oven at 120 ^{o}C for 10 minutes.
3. The PZT layer is then placed in a gold sputtering machine and coated with gold on both sides. The gold sputtering machine is as shown below.

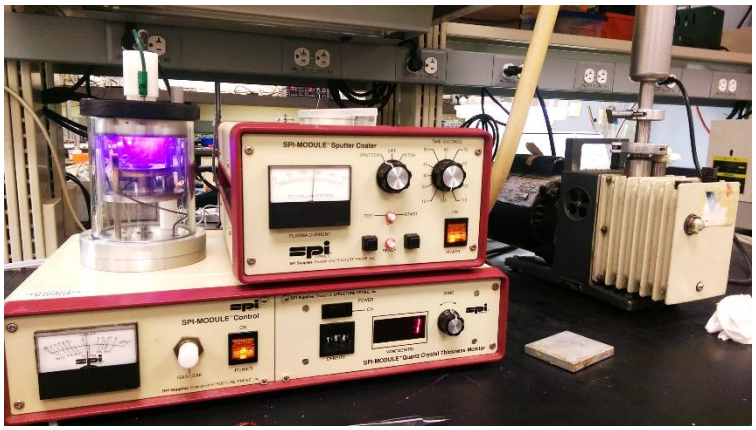


Fig 27: A gold sputtering machine

a. The gold sputtering machine is connected to a supply of argon cylinder and a vacuum pump.

b. The first step involves placing the PZT in the chamber in the target zone and securing all the air valves and the vacuum pump is switched on. This sucks out the atmospheric air and the pressure inside the chamber falls in the milli-Torr range. The setup is left untouched for about 15 minutes.

c. The argon cylinder valve is now opened and a regulator that is attached maintains the pressure at about 5 atm. The gas enters the setup and using the release knob, the argon gas is introduced into the chamber. All this while, the vacuum pump is still on and is left as such till the end of the process. The knob is adjusted to an extent where the influx of Argon surpasses the out flux and maintains a pressure of about 2 milli-Torr in the chamber. Sufficient time is allowed to make sure there is no atmospheric air inside the chamber and that argon successfully flushes and occupies the chamber.

d. The sputtering machine is now switched on for about 120 seconds and the gold is coated onto the device. This step is repeated once again to get a thicker coating.

e. Once the sputtering process is completed, the setup along with the vacuum pump is stopped. The valves are opened to neutralize the negative pressure in the chamber and the PZT is removed.

f. All the above steps are repeated to get a similar coat on the other side of the PZT material.

4. After the PZT is gold coated, it is then placed in the KOH solution to remove the photoresist, thereby removing the gold above to create a distinct channel. The PZT is then cleaned in deionized water and dried

A step by step illustration from cut to gold coating with channels

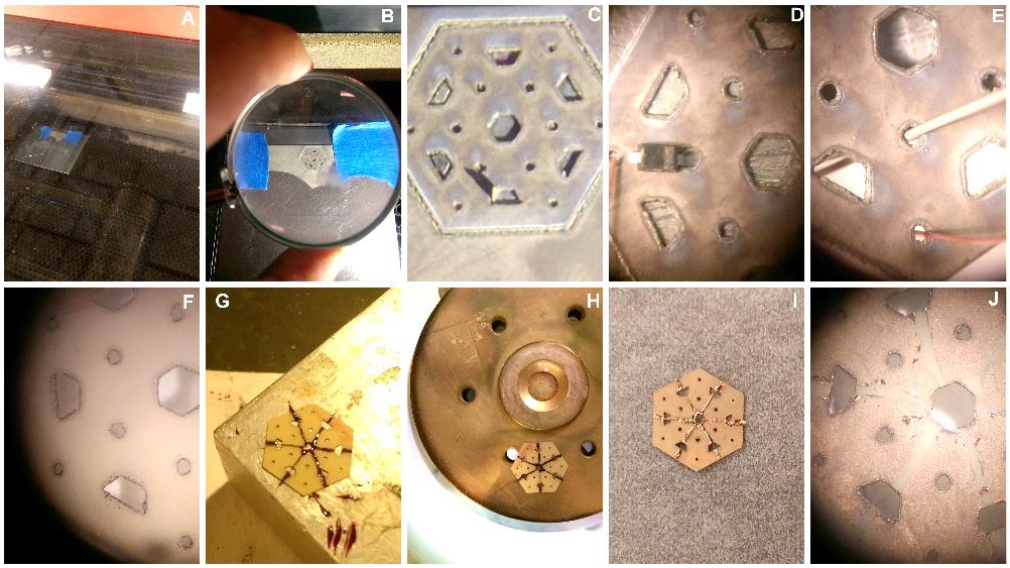


Fig 28: A: PZT cut in the laser machine, B: Inspecting the PZT for proper cuts through a lens, C: The final cut PZT it ready to be disengaged from the parent base, D: The diode placed

5. The PZT material is now ready for making the final device.

Making of the Final 2 Channel Gold Coated Device

For this procedure, a silver conductive epoxy is prepared similar to the epoxy mentioned in section 3.2. A non – conductive epoxy is made from Epoxy technology 353 – 3M by mixing part A and part B in the ratio 10:1 on a micro weighing scale.

A 6mm copper wire with an insulating coating is soldered onto the anode of the diodes. This is done for all the diodes to be used in making these devices. The diode (Schottky diode SMS 7630-079 LF package from Skyworks solutions inc. which has a bias voltage of 130 mV) is then placed on either side of the channel on top of the holes on the negative side of the PZT. The holes were created with respect to the diode dimensions in consideration. The cathode of the diode is

connected to the negative side of the PZT using conductive epoxy on top of the 0.35mm diameter hole and is baked in an oven for 5 minutes at 120^{o}C. The copper wire connected to the diode is made to go through the 0.25 diameter hole onto the other side and attached using the epoxy to the positive side of the PZT and baked again. The diodes are now firmly attached.

The electrodes are now introduced to the 0.35 mm diameter hole from the positive side and attached using conductive epoxy carefully in order to avoid shorting to the positive side. The device is again baked to make sure the contacts are firm.

The non-conductive is now introduced onto the negative side of the PZT with the diodes and baked for 15 mins at 120^{o}C. The device is removed and is allowed to cool for 20 minutes for the epoxy to harden. On the positive side, the epoxy is placed on the 0.35mm holes to electrically isolate the conductive epoxy attached to the negative layer of the PZT and is baked again.

3.8.2. Nickel Coated Devices

Making of the Nickel coating devices involves fewer steps and smaller scale devices which makes their handling more of a task.

Once the PZT is cut with the channel made by the laser itself, a micro syringe is used to flush the acid through the channel to further remove any remnant nickel metal.

The further steps in attaching the diodes and the electrodes are similar to the gold coated devices. Both single channel and 2 channel devices were constructed.

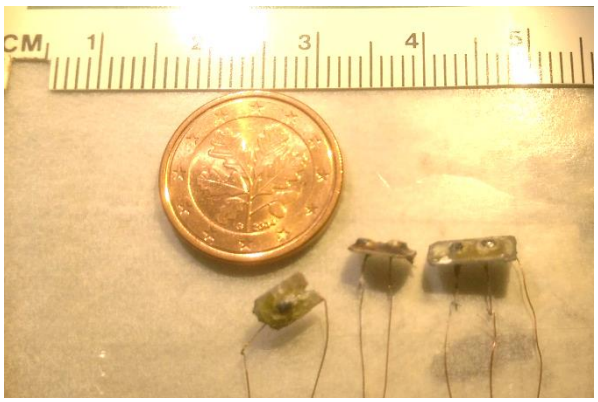


Fig 29: Photographs of the final devices. Starting from left, 1 channel nickel device, 2 channel gold device and 2 channel nickel device.

3.9. Capacitance Calculations of PZT Neurostimulators

The capacitance of all the base materials of PZT devices were measured using a capacitance meter to calculate the output port impedances. As each of the piezoelectric layer is nothing but a PZT ceramic with two metal layers, it is similar to that of a capacitor and has no significant resistive or inductive components. So the formula for the capacitive reactance is used.

$$X_C = \frac{1}{\omega C} = \frac{1}{2\pi f C}$$

Where Xc = Capacitive reactance

F= frequency of the input pulse

C = Capacitance of the base material

3.10. Bench Test of Neurostimulators for Maximum Voltage Generated Under Tissue Conductivity

A series of bench tests were performed to evaluate the maximum output generated by these devices. They were tested in two different setups, The Short- Pulses Pulser/Receiver and the Tone burst ophir setup.

Short- Pulses setup input signal:

The input signal from the Panamterics Pulser/Receiver was a 100 V pulse with 100 uJ of energy.

Tone Burst Ophir Setup Input Signal

The input signal to the transducer was a 2.5 uS long pulse that is modulated with a resonant frequency signal of 2.25 MHz from a signal generator. The inter pulse period was about 50 ms .

Two different measuring probes were connected to both the channels of the device and were then connected to the individual channels of the CRO.

Preparation of Different Conductivity Solutions

For achieving 2 mS/cm conductivity, about 9gms of common salt was diluted with 1000 ml of Deionized water and mixed in a conical flask and stored. Also a saturated solution of salt solution

was prepared by constantly adding common salt to 1000 ml of deionized water and heated to 50 ^{o}C to get a highly saturated mixture. To achieve the different conductivities required for the different experiments 1000 uL of the saturated solution was added to deionized water with constant measuring of the conductivity using a digital conductivity meter.

Experimental Procedure

The devices were held on the stage in the water bath with the longer edge running parallel to the X axis of the micro manipulator and the shorter edge on the Y axis. All the channels on all the devices had insulted copper wires soldered onto them with the insulation of the copper wires removed in the ends to create the metal contact and provide contact for the measuring probes to be attached. The bath is then filled with distilled water and the electrodes are drawn to the glass jar adjacent to it, which holds the conductive solution, simulating the tissue conductivity environment. A conductive meter constantly reads the conductivity of the solution to make sure it isn't a variable. The measuring probes pick up the output signal generated across the electrodes in the conductive solution.

The conductive solution used in these experiments ranged from 0mS/cm(No Load) to 1.7 mS/cm, 2 mS/cm and 20 mS/cm to simulate the conductivity of the peripheral nerve, Brain gray matter and Cerebrospinal fluid respectively.

A 2.25 MHz transducer was connected to the transducer station connected to the micro manipulator which moves in X,Y,Z axis and it is connected to the Panametrics Pulser/ Receiver in the first experiment and to the Linear Power amplifier for the second experiment.

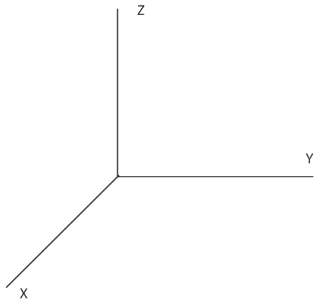


Fig 30: Micro manipulator axis

The Z axis was set at 1.25” from the surface of the devices, which is the depth specified by the manufacturer. The manipulator was moved in the X and Y axis and the maximum output was recorded.

Short- Pulse Response Setup Output Recording

Since the Short- Pulse response setup has a single receiver probe, when testing more than one channel, the probe was individually attached to the different channels one at a time and the manipulator was adjusted to record the maximum output. The values were then recorded in table 6 for PVDF devices and table 9 for PZT devices.

Tone Burst Setup Output Recording

In the Tone burst setup, all the channels were simultaneously monitored on the CRO. It must be highlighted at this point that only the device stage settings were common in both the setups. The input settings and the CRO probe and External trigger settings changes with the two experiments accordingly as described in the initial mentioning of the two setups in section 3.3

These tests were performed for all the devices manufactured and all the channels were simultaneously monitored and the maximum output in the channels for no load and in a conductive solution of 1.7mS/cm were recorded and compiled in the table 7 for PVDF devices and table 10 for PZT devices.

The maximum output was checked in a no load and as well as in a conductive solution mimicking the tissue conductivity.

3.11. Demonstration of Multichannel Functionality of the Neurostimulators

To validate the multichannel functionality the following study was undertaken.

From the PVDF devices, a 3 mm X 1mm 2 channel, 7 mm X 1 mm 2 channel Series anodic devices and 7 mm X 1mm 2 channel parallel interconnect series device was chosen. Long insulated coated copper wires with around 2 mm of insulation removed at the edges were soldered onto the electrodes to provide connectivity for measurements.

From the PZT devices, 6 mm X 4 mm gold plated dual channel device and a 7 mm X 4 mm plain nickel 2 channel device was chosen and the same steps were repeated as with the PVDF devices.

The setup of the device on the stage and the input settings are the same as discussed in the previous section 3.10 which is the Tone burst setup. A 2.25 MHz transducer was connected to the transducer station connected to the micro manipulator which moves in X, Y, Z axis and it is connected to the Linear Power amplifier. The setup is similar to Tone burst setup shown in the experiments done earlier.

The input signal to the transducer was a 25 uS long pulse with a carrier frequency signal of 2.25 MHz from a signal generator. The inter pulse period was about 50 ms.

Two different measuring probes were connected to both the channels of the device immersed in a conductive solution of 1.7 mS/cm that provided a load similar to the tissue and were then connected to the individual channels of the CRO.

The Z axis is set at 1.25” from the surface of the device which is the focal depth prescribed by the manufacturer. The micro manipulator is then moved in the X axis and simultaneously on the Y axis. At a specific point, the device gives a maximum output.

The Y axis is then fixed and the micromanipulator is then moved along the X axis, moving the ultrasound transducer and the beam along. The output from both the channels are simultaneously monitored and recorded.

Similarly at the junction where there is maximum output, the X axis if fixed and the output from both the channels were simultaneously recorded.

The Z axis is then changed to two different heights, 0.85” and 1.48” from the surface of the device and the maximum output from the device was recorded at for a fixed X and Y position. This procedure was repeated for all the four devices.

3.12. Current Generated in the Nickel and Gold Plated 2 Channel Devices

The Nickel and gold plated devices were chosen to perform a study to determine the current generated by these devices. The reason for choosing these particular devices out of all the devices will be discussed in the results section.

These devices were setup on the stage and the experimental procedure was the same as mentioned in the previous section 3.11 with the same input settings.

The micro manipulator was adjusted to have a maximum output from the device on one particular channel.

A differential load setup in the form of known resistors on a breadboard was connected in parallel to the output electrodes of the device and the output was measured as a factor of the varying load. This was repeated for both the devices and the values recorded.

3.13. Output Dependency of the Devices with Respect to the Conductivity of the Solution

The output of the devices can be a function of the conductivity of the solution between the measuring electrodes. A study was performed to see the performance of two devices chosen in random and tested for its output vs conductivity.

The devices 3mm X 1mm 2 channel series anodic and 2 channel nickel device was chosen. They were setup on the stage with the Tone burst settings as mentioned in section 3.11. The manipulator was adjusted to get a maximum output on one of the channels. The device electrode extensions were soaked in the distilled water container. The conductivity was increased by adding 1000uL of saturated common salt solution little by little and stirred and let to settle for 5 secs and

the output was then recorded. A conductivity meter was measuring the conductivity continuously. Results shown in Fig 53, 54.

3.14. Ultrasound Acoustic Power and Focal Spot Experiment to Determine Acoustic Power Density

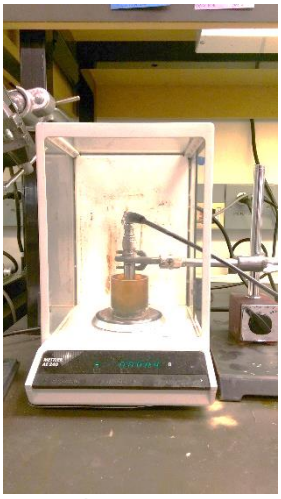


Fig 31: On the left: The force balance experiment to measure the Acoustic power of the 2.25 MHz transducer

It is essential to estimate the acoustic power density to adhere to the FDA limits. The acoustic power density for a focused transducer is determined by dividing the acoustic power by the focal spot for a focused transducer.

The acoustic power was measured by the setup in the figure 31. The 2.25 MHz transducer was connected to the Linear Power amplifier with the standard Tone burst input settings, though with the pulse interval being reduced from 50 ms to 1 ms to get an almost continuous waveform. The transducer was suspended with the help of a holder onto to a bath filled with water whose base is made of a highly absorptive medium. The weighing scale used was a Mettler AE 240 which has a sensitivity of 0.1 mg. The whole setup was left undisturbed for a day to remove the possible chances of drift.

The following day the transducer was powered by the Linear Power amplifier and the change in mass was recorded. It is then inputted into the equation below to determine the acoustic power [45].

$$P = \frac{\Delta m \cdot g \cdot c}{1+R^2}$$

Where P is the acoustic power Δm is the change in weight caused by the ultrasound beam, g is the gravity, c is velocity of ultrasound waves in water and R is the reflection coefficient of the target. In this case, the target being a sponge, it is considered to be highly absorptive and hence the R=0.

The focal spot area was estimated to be around at 0.30 mm^2. The Acoustic density was calculated by dividing the acoustic power with the focal spot area.

3.15. Impedance Measurements of the Different Electrodes Used: Electrode-Electrolyte Interface

The impedance of the electrodes when they are in the electrolyte (conductive medium) also plays an important role and gives an understanding on the behavior when placed in the tissue. For this study an electrochemical method using CH instruments was used. All the various electrodes used in the making of the device (PT/IR of various thicknesses) and the copper wires were evaluated. These electrodes were evaluated against the standard Ag/AgCl electrode in a Saline solution.

Once the setup is readied, the proprietary software is run to generate bode plots, as shown in the figure 32 to determine the impedance of the electrode electrolyte impedance at different frequencies. This experiment was performed for 3 iterations on each electrode to check for consistency.

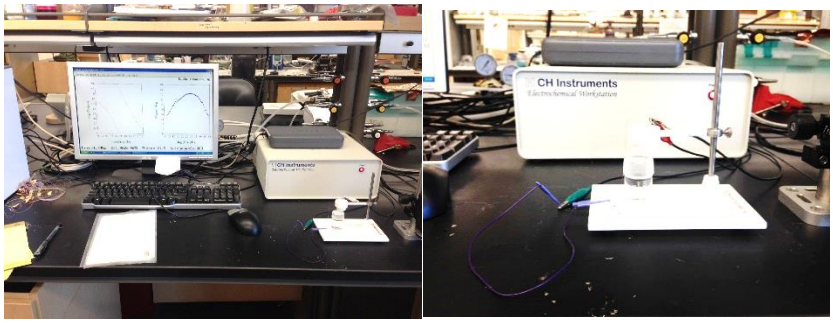


Fig 32: Photograph of the electrochemical setup

The effect of chronic intra cortical microstimulation on the electrode- electrolyte (tissue) interface has been a subject to concern. Several studies [46] were undertaken and it was proved that chronic ICMS has only a minor effect on the electrode- tissue interfaces and thus it has been established as a viable means to convey sensory feedback in neuro prosthetics.

Also injection of high currents through the contacts can be a challenge for electrode – electrolyte interface. The voltage is limited by the distance between the electrodes and can determine whether the current is injected by faradic or capacitive mechanisms as stated in this study [24].

However, several materials have been investigated in the near past for high charge injection capacity (CIC). For anodic stimulation, Iridium oxide contacts are a better option. For a capacitive mechanism, tantalum oxide, titanium nitride and poly (3,4 –ethylenedioxythiophene) (PEDOT) has been suggested. By using such coatings, the contacts can be made smaller without exceeding the CIC.

CHAPTER 4

RESULTS

4.1. In-Vitro Performance of a Piezoelectric Element to Ultrasound

The performance of a piezoelectric element follows the piezoelectric principle. When a mechanical force is applied charge is generated. The output of the piezoelectric element to a ultrasound tone burst is as shown below.

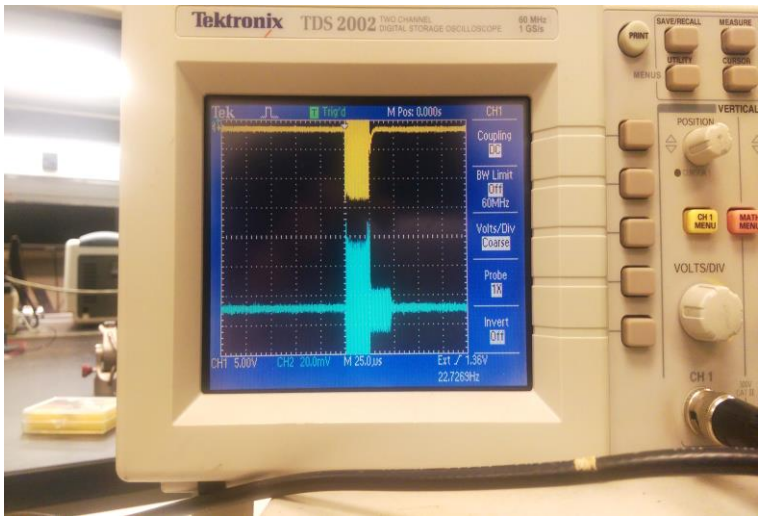


Fig 33: Output of a piezoelectric element to ultrasound

The output is an AC signal as the piezoelectric material experience a pressure-rarefaction force of the ultrasound wave. The sign of the electrical charge generation corresponds to the direction of the force.

4.2. Bench Tests of PVDF Test Elements

Several bench tests were performed on the test materials using different setups to understand the performance of these materials.

4.2.1. Short- Pulse Response

The conductivity of the medium was 0mS/cm which means it was a no load condition

The different test materials tested were

2mmX 1mm 1layer, 2 layer, 3 layer

3mm X 1mm 1layer, 2 layer, 3 layer

The tests were conducted on a differential load setup using different transducers (2.25 MHz, 5 MHz, 20 MHz). At lower loads the voltage drops and gradually rises at increasing loads and becomes a constant resembling the voltage across an open circuit.

It is to be noted that all the voltages measured are peak to peak. All Short- Pulse setup experiments have a 20dB gain on the output, which means the effective output is 1/10 of the output recorded.

Also the recorded output is substantially damped due to the capacitance of the tweezer which is around 7pF coupled with the probe and setup capacitance which is around 155 nF. Therefore taking this damping factor and the gain of 20dB, the outputs are deliberated upon.

A sample pulse response output is as below

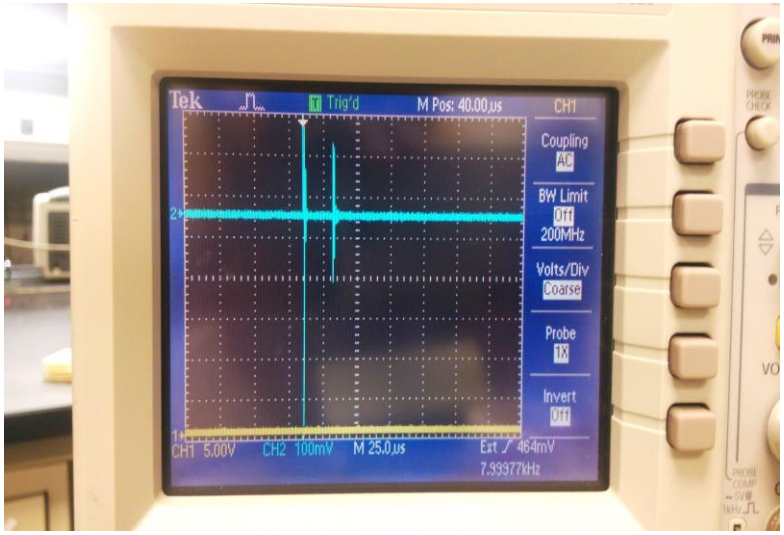


Fig 34: Short- Pulse output of a Piezoelectric element

The signal measured on the left is the transmitter drive signal artifact. The second pulse is the electrical voltage detected from the device.

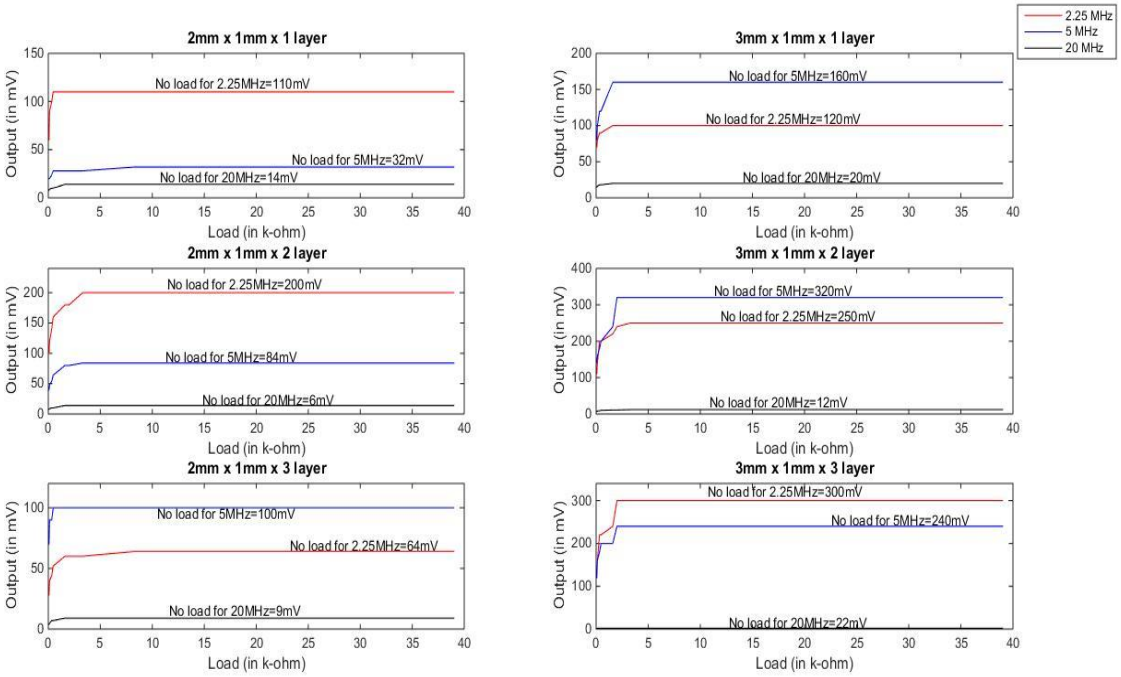


Fig 35: Performance of 2mmX 1mm 1layer, 2 layer, 3 layer and 3mmX 1mm 1layer, 2 layer, 3 layer for a Short- Pulse setup across different transducers

In all the experiments above, the 2.25 MHz transducer produced a higher output in the 2mm X 1mm devices except for the 3 layer device. This is due to the fact that the wavelength of the beams of the different transducers.

In the 3mm X 1mm devices the 5 MHz transducer produced a higher output in the devices except for the 3 layer device.

4.2.1. (i). D33 Vs D31 Test on a 3mm X 1mm 2 Layer PVDF Test Device

An experiment was also done to understand the amount of charge (output) generated due to the incidence of the ultrasound on the different poling sides of the piezoelectric element. The input settings was similar to the setup in the above experiment. A 2.25 MHz transducer was used.

The peak to peak voltages were recorded as follows

D33 is around 130 mV and D31 is around 8 mV

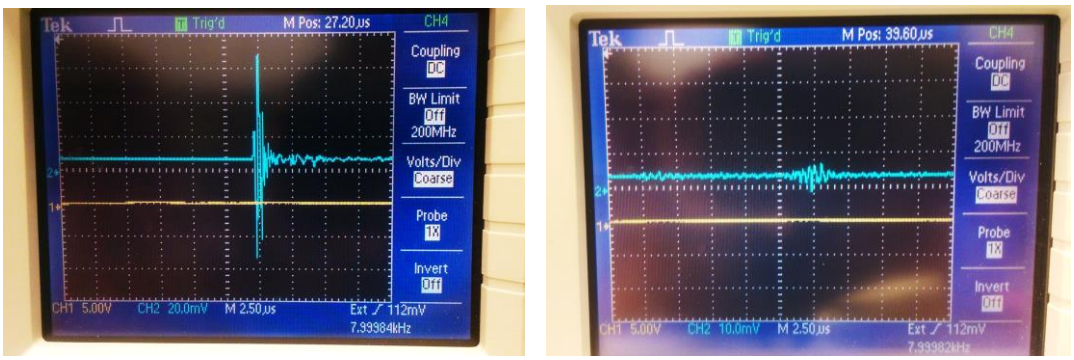


Fig 36: D33 vs D31 measurement in a 3mm X 1mm 2 layer PVDF test material

4.2.2. Tone Burst Response

The conductivity of the medium was 0mS/cm which means it was a no load condition and a differential load setup with resistors was connected across the measuring probes and the devices were tested for their performance across different loads with respect to different transducers (2.25 MHz and 5 MHz) and the output was recorded

The different test materials tested were

2mmX 1mm 1layer, 3 layer

3mm X 1mm 1layer, 3 layer

A sample output of the Tone burst setup on a piezoelectric element is as below

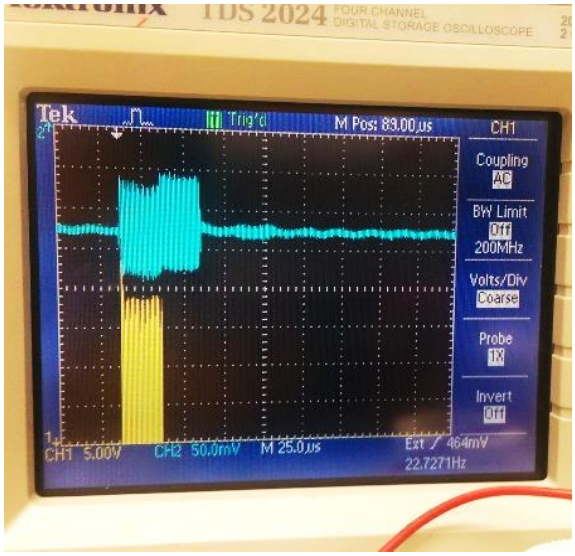


Fig 37: Output of a Piezo electric element under Tone burst setup

The output is seen in the blue channel immediately after the input artifact.

It must be noted that there are still capacitive losses due to the tweezer and the setup capacitance. However, there is no gain added and the recorded value is the final value.

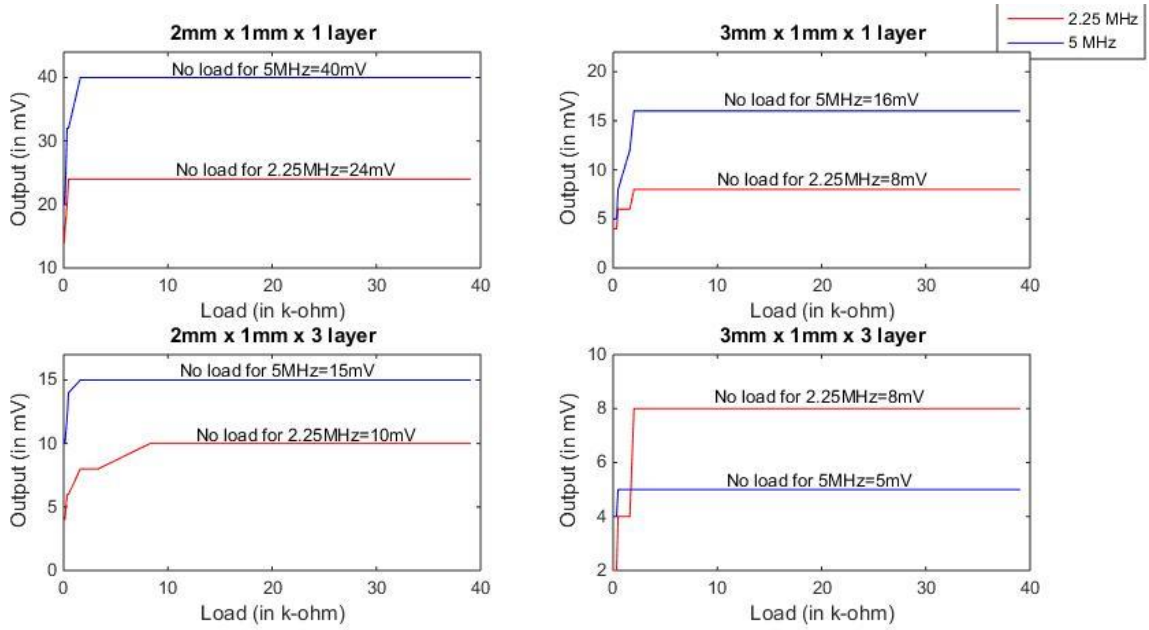


Fig 38: Performance of 2mmX 1mm 1layer and 3 layer and 3mmX 1mm 1layer and 3 layer for a Tone burst setup across different transducers

In all the experiments above the 5 MHz transducer produced a higher output and in the 3mmX 1mm 3 layer the 2.25 MHz transducer produced a higher output.

4.2.2. (i) Output Dependence on the Drive Voltage to the Transducer

A comparative study was undertaken to understand the dependence of the output on the drive voltage to the transducer. A 2mmX1mm 1 layer device was powered by a 2.25 MHz transducer.

Two different drive voltages 20 V and 35 V were applied on the transducer and the output was measured across different loads. The output is a maximum when the drive voltage to the transducer is also a maximum.

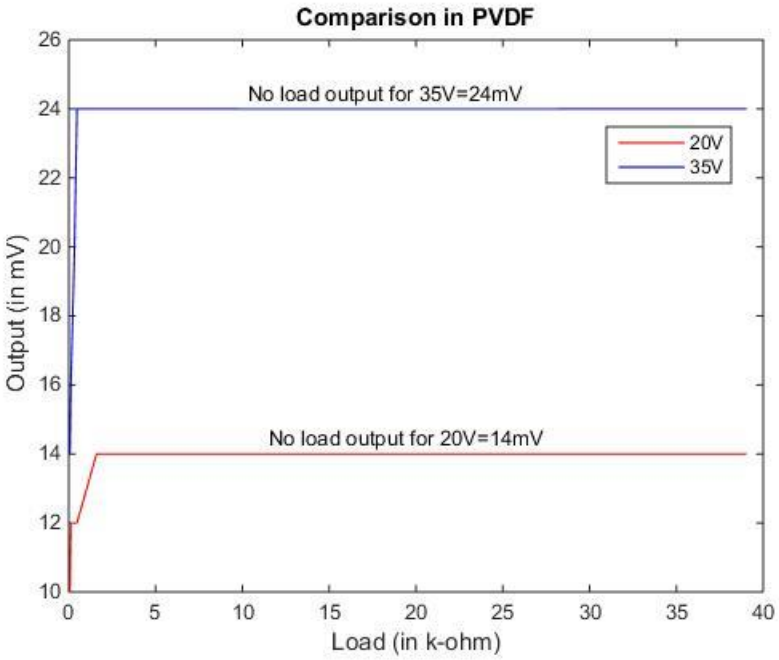


Fig 39: Performance of 2mmX 1mm 1layer for a Tone burst setup with a 2.25 MHz transducer driven by different voltages

4.3. Capacitance of PVDF Test Materials

The capacitance of the PVDF materials is as follows

Material	Capacitance
2mm X 1mm 1 layer	2.5 pF
2mm X 1mm 2 layer	14.5 pF
2mm X 1mm 3 layer	24.3 pF
3mm X 1mm 1 layer	4 pF
3mm X 1mm 2 layer	24 pF
3mm X 1mm 3 layer	36 pF

Table 4: Capacitance of PVDF test materials

4.4. Bench Tests of PZT Test Elements

4.4.1. Short Pulse Response

The conductivity of the medium was 0mS/cm which means it was a no load condition

The different test materials tested were

2.5 mm X 4 mm X 0.305 mm and 5mm X 4 mm X 0.305 mm

The tests were conducted on a differential load setup using different transducers (2.25 MHz, 5 MHz, 20 MHz). At lower loads the voltage drops and gradually rises at increasing loads and becomes a constant resembling the voltage across an open circuit.

It is to be noted that all the voltages measured measured from peak to peak. All Short-Pulse setup experiments have a 20dB gain on the output, which means the effective output is 1/10 of the output recorded.

The devices had wires soldered onto it, hence no need for the tweezer setup which means there is no damping due to the capacitances.

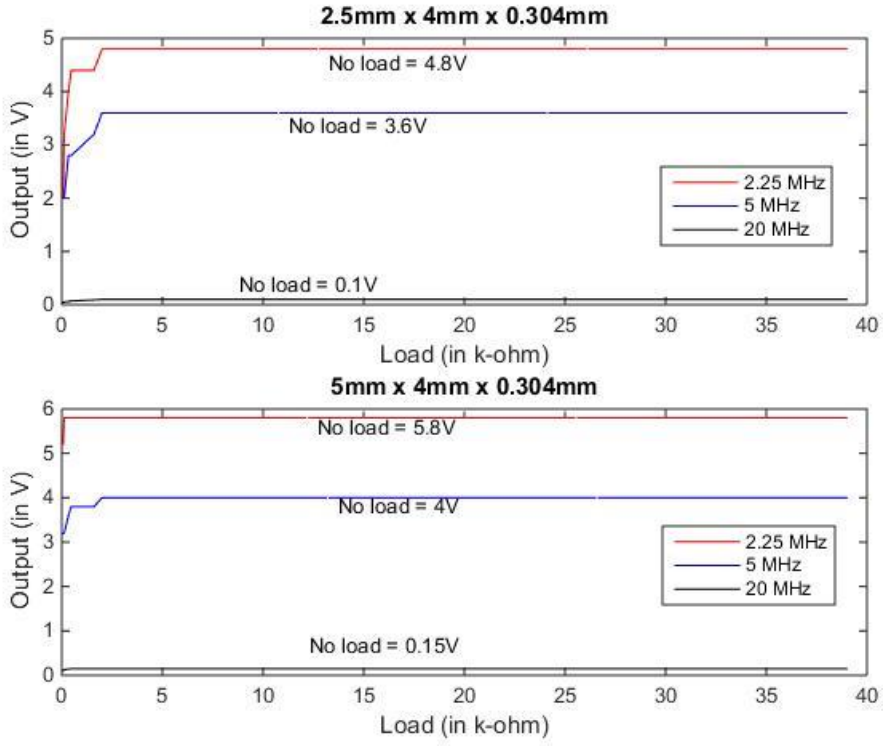


Fig 40: Performance of 2.5mmX 4mm X 0.305 mm and 5mmX 4mm X 0.305 mm for a Short-Pulse setup across different transducers

In the above experiments the 2.25 MHz transducer generated the maximum output in the devices

4.4.1. (i). Tweezer Vs Wired Device

To understand the effect of the capacitance of the tweezer and the wired device this experiment was conducted on a 2.5mmX 4mm X 0.305 mm device in a Short- Pulse setup using a 2.25 MHz transducer.

The outputs measured were as follows.

Using tweezers: No load output voltage was 4 V

Direct wires connected to probe: No Load voltage was 18 V

4.4.2. Tone Burst Response

The conductivity of the medium was 0mS/cm which means it was a no load condition and a differential load setup with resistors was connected across the measuring probes and the devices were tested for their performance across different loads with respect to different transducers (2.25 MHz and 5 MHz) and the output was recorded

The different test materials tested were

2.5 mm X 4 mm X 0.305 mm and 5mm X 4 mm X 0.305 mm

It must be noted that there are no capacitive losses due to the removal of the tweezer setup for measuring. They just merely provide a mechanical support. Also, there is no gain added and the recorded value is the final value.

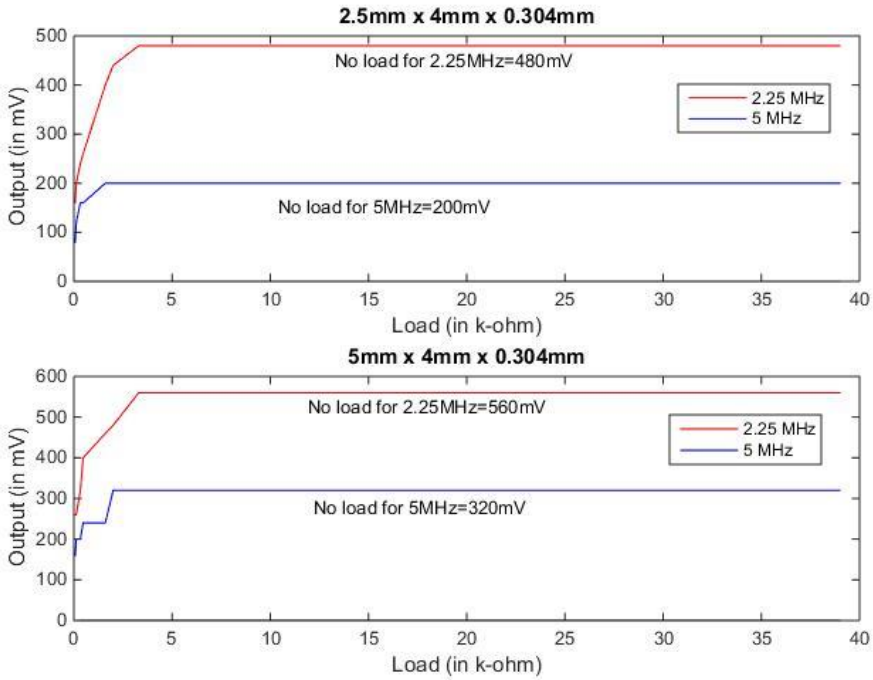


Fig 41: Performance of 2.5mmX 4mm X 0.305 mm and 5mmX 4mm X 0.305 mm for a Tone burst setup across different transducers

It was noted that the 2.25 MHz produced a higher output from the devices.

4.4.2. (i) Output Dependence on the Drive Voltage to the Transducer

A comparative study was undertaken to understand the dependence of the output on the drive voltage to the transducer. A 2.5 mm X 4mm x 0.305 mm PZT was powered by a 2.25 MHz transducer.

Two different drive voltages 20 V and 35 V were applied and the output was measured across different loads.

It is demonstrated the output of the device is directly proportional to the drive on the transducer.

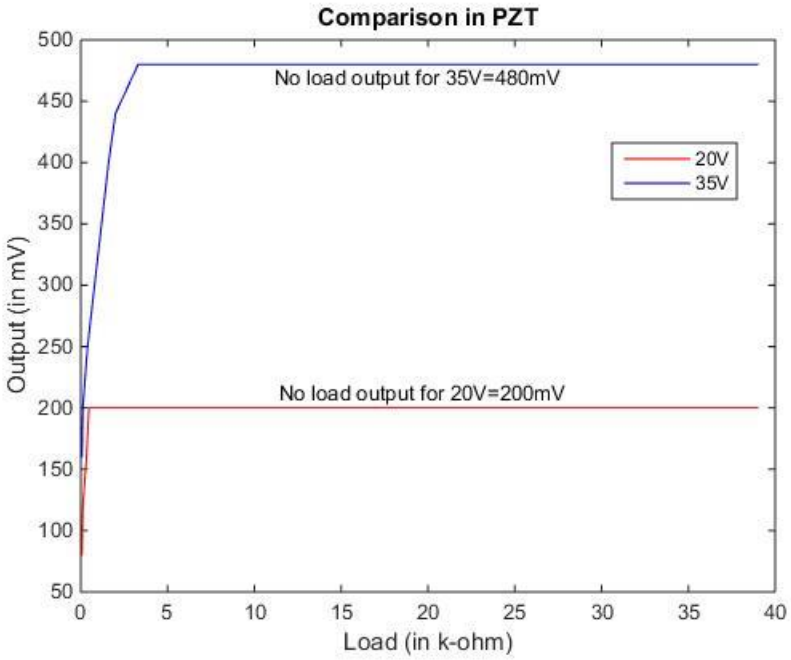


Fig 42: Performance of 2.5mm X 4mm X 0.305 mm PZT device on a Tone burst setup with a 2.25 MHz transducer driven by different voltages

4.5. Capacitance of the PZT Test Materials

Material	Capacitance
2.5mm X 4mm X 0.305 mm	450 pF
5mm X 4mm X 0.305 mm	830 pF

Table 5: Capacitance of PZT test materials

4.6. Bench Test for Devices to Check for their Maximum Voltages

4.6.1 PVDF Neurostimulators

4.6.1. (i). Panametric Short Pulse Response

There is gain of 20 dB while recording. The actual output is 1/10 the recorded output. All the devices are wired, hence no capacitive losses. The conductivity of the solution was around 1.7 mS/cm.

Device	Maximum Voltage in (mV)			
3mm X 1mm X 5 layer 1 Channel Series anodic	700			
3mm X 1mm X 5 layer 2 Channel Series anodic	300		340	
7mm X 1mm X 5 layer 4 Channel Series anodic	200*	100*	480	640
7mm X 1mm X 5 layer 1 Channel Series anodic	360			
7mm X 1mm X 5 layer 2 Channel Series anodic	560		360	
3mm X 1mm X 3 layer 2 Channel Series Cathodic	360		1080	
3mm X 1mm X 5 layer 2 Channel Series Cathodic	40		100	
3mm X 1mm X 5 layer 1 Channel Parallel Anodic	120			
7mm X 1mm X 5 layer 1 Channel Parallel anodic	600			
7mm X 1mm X 5 layer 2 Channel Parallel anodic	600		760	

*Table 6: Short- Pulse bench test of PVDF devices, *damaged channels*

4.6.1. (ii). Tone-Burst Response

The conductivity of the solution was around 1.7 mS/cm

No gain was added and the recorded voltage was the actual voltage

Device	Maximum Voltage in (mV)			
3mm X 1mm X 5 layer 1 Channel Series anodic	20			
3mm X 1mm X 5 layer 2 Channel Series anodic	80		120	
7mm X 1mm X 5 layer 4 Channel Series anodic	20*	3*	80	80
7mm X 1mm X 5 layer 1 Channel Series anodic	100			
7mm X 1mm X 5 layer 2 Channel Series anodic	60		20	
3mm X 1mm X 3 layer 2 Channel Series Cathodic	100		150	
3mm X 1mm X 5 layer 2 Channel Series Cathodic	60		70	
3mm X 1mm X 5 layer 1 Channel Parallel Anodic	60			
7mm X 1mm X 5 layer 1 Channel Parallel anodic	80			
7mm X 1mm X 5 layer 2 Channel Parallel anodic	80		80	

*Table 7: Tone burst bench test of PVDF devices, *damaged channels*

To be noted, the maximum output of all the devices were bench tested with copper electrodes soldered to the devices as initial floating electrode setup led to a reduced output due to the losses by the presence of liquid between the measuring probe and the device electrodes. During the process of soldering on PVDF devices, at the end of it some of the devices showed no response on some of the channels due to what is suspected to be a result of depolarization. This is due to the fact that sometimes the soldering rods reached temperatures in excess of 400 ^{o}C.

Sample Tone burst output of a 7mm X 1mm X 5 layer 4 Channel Series anodic device.

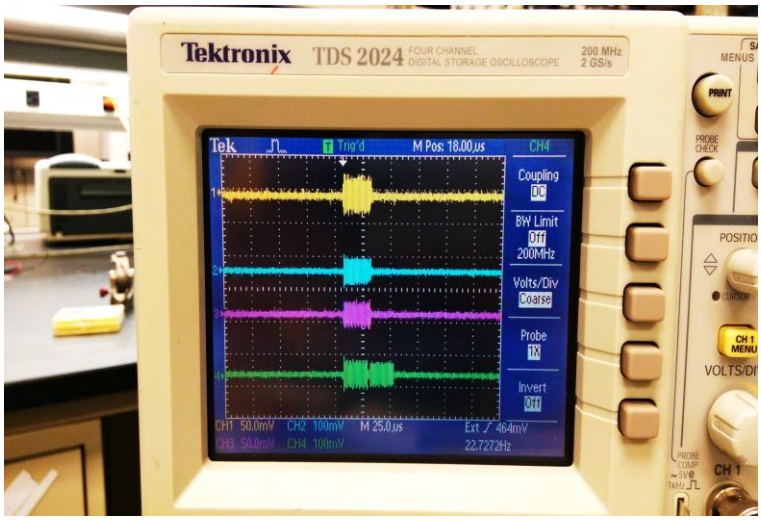


Fig 43: Simultaneous four channel monitoring in a 7mm X 1mm X 5 layer 4 Channel Series anodic device in a Tone burst setup

One will notice that the 4th channel is distinctly active while the rest of the channels are inactive. Also the output seen here is an AC voltage generated by the PVDF layers.

4.6.1. (iii) Capacitance Calculations of Both Serial and Parallel Devices

Inputting this into the reactance equation determines that the parallel devices will have considerably lower output port impedances than compared to the series interconnect devices as the reactance is inversely proportional to capacitance.

Device	Capacit-ance	Output Port impedance ohms Freq = 2.25 MHz
7mm X 1mm 5 layer 2 channel Series Anodic	1.1 pF	64 K ohms
7mm X 1mm 5 layer 3 channel Series Anodic	1.1pF	64 K ohms
7mm X 1mm 5 layer 4 channel Series Anodic	1.1pF	64 K ohms
3mm X 1mm 5 layer 1 channel Parallel Anodic	6 pF	11 K ohms
7mm X 1mm 5 layer 1 channel Parallel Anodic	18 pF	3 K ohms

Table 8: Capacitance of PVDF fabricated devices

This table shows that the parallel interconnect devices have lower output port impedance in comparison with the series interconnects.

4.6.2. PZT Neurostimulators

4.6.2. (i). Short Pulse Response

There is gain of 20 dB while recording. The actual output is 1/10 the recorded output. All the devices are wired, hence no capacitive losses

The conductivity of the solution was around 1.7 mS/cm

Device	Maximum voltage in mV	
2.5 mm X 4 mm X 0.305 mm 1 channel nickel device	600	
6 mm X 4 mm X 0.305 mm 2 channel gold device	600	420
7 mm X 5 mm X 0.305 mm 2 channel nickel device	800	600

Table 9: Short Pulse bench test of PZT devices

4.6.2. (ii). Ophir Tone Burst Response

The conductivity of the solution was around 1.7 mS/cm

No gain was added and the recorded voltage was the actual voltage

Device	Maximum voltage in mV	
2.5 mm X 4 mm X 0.305 mm 1 channel nickel device	200*	
6 mm X 4 mm X 0.305 mm 2 channel gold device	170*	110*
7 mm X 5 mm X 0.305 mm 2 channel nickel device	170*	90*

Table 10: Tone burst bench test of PZT devices

*Note: These are rectified DC voltages from the diode. The actual voltage generated is much higher.

Sample tone burst response output of a 7 mm x 5 mm x 0.305 mm 2 channel nickel device.

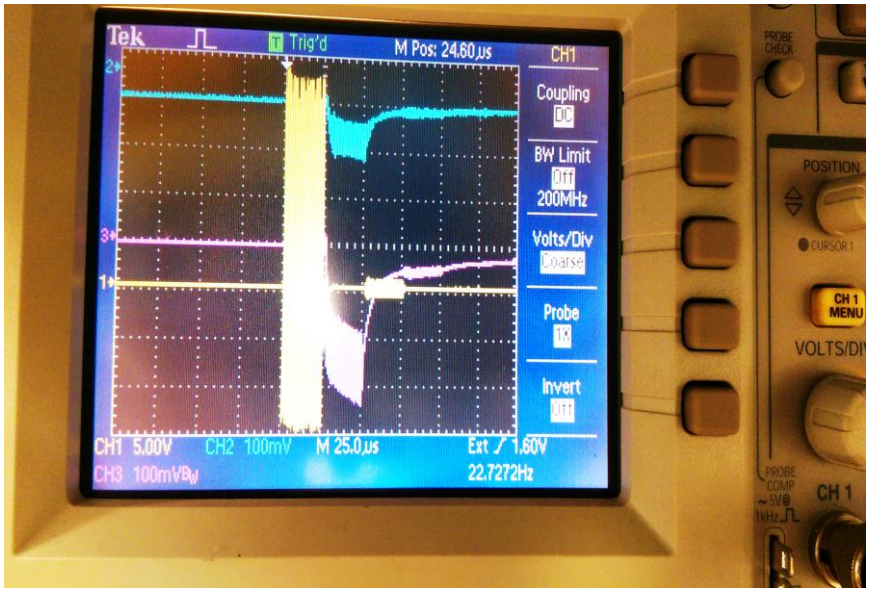


Fig 44: Simultaneous dual channel monitoring in a 7 mm X 5 mm X 0.305 mm 2 channel nickel PZT device in a Tone burst setup

One will notice that the output in the second channel is a rectified DC output with an amplitude of 170 mV and the 1st channel has an output of about 70 mV rectified DC. The 2 channels are simultaneously active, however each of them peaks at a particular spatial distance of the beam on the device and this make it uniquely multichannel.

4.7. Demonstration of Multichannel Functionality in PVDF and PZT Neurostimulators

The goal of these tests is to determine the effect of moving the transducer focal spot across the piezoelectric devices.

As the transducer focal spot moves across the device, the 2 channels are activated and the voltage increases and drops as the beam crosses over. The voltages when plotted with respect to the axis movement yields a curve like in the figure 47.

4.7.1. PVDF Neurostimulators

4.7.1.(i) 3mm X 1mm 5 Layer Series Interconnect, 2 Channel Cathodic Stimulation Device

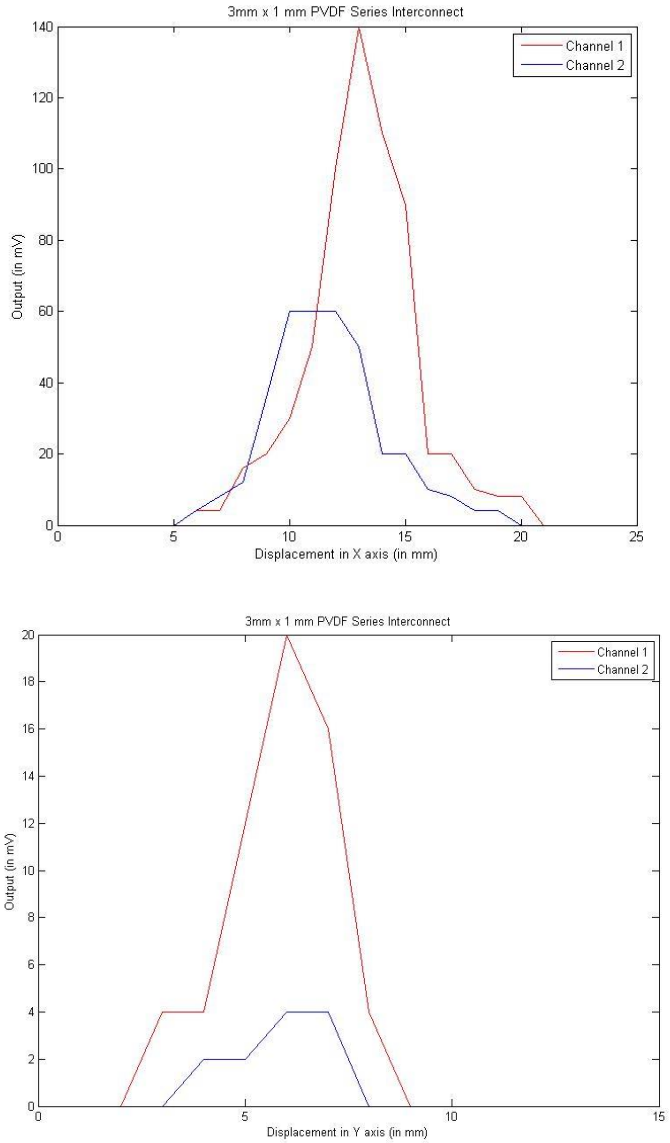


Fig 45: X axis displacement vs Voltage in both channels and Y axis displacement vs Voltage in both channels for a 3mm X 1mm 5 layer series interconnect, 2 channel cathodic stimulation PVDF device

Different Z Axis Height

1.25” – 20 mV and 4 mV were the maximum voltages in CH1 and CH 2 respectively

0.86” – 16 mV and 4 mV were the maximum voltages

1.41” – 16 mV and 0 mV were the maximum voltages

4.7.1.(ii) 7mm X 1mm 5 Layer Series Interconnect, 2 Channel Cathodic Stimulation Device

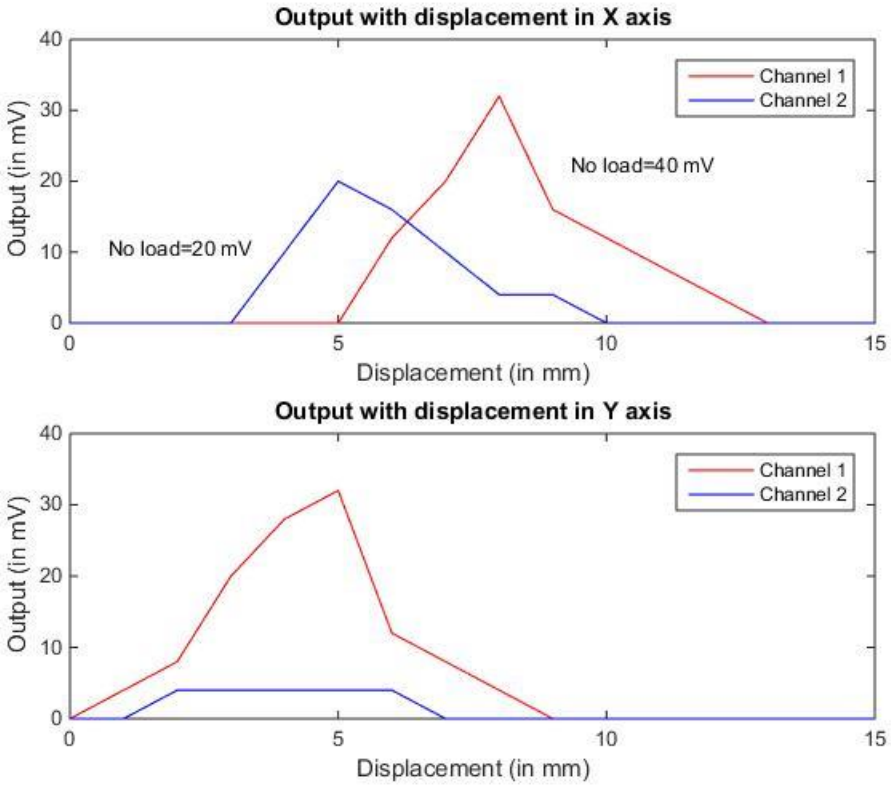


Fig46: X axis displacement vs Voltage in both channels and Y axis displacement vs Voltage in both channels for a 7mm X 1mm 5 layer series interconnect, 2 channel cathodic stimulation PVDF device

Different Z Axis Height

1.25” – 32 mV and 4 mV were the maximum voltages in CH1 and CH 2 respectively

0.86” – 16 mV and 4 mV were the maximum voltages

1.41” – 24 mV and 8 mV were the maximum voltages

4.7.1.(iii) 7mm X 1mm 5 Layer Parallel Interconnect, 2 Channel Cathodic Stimulation Device

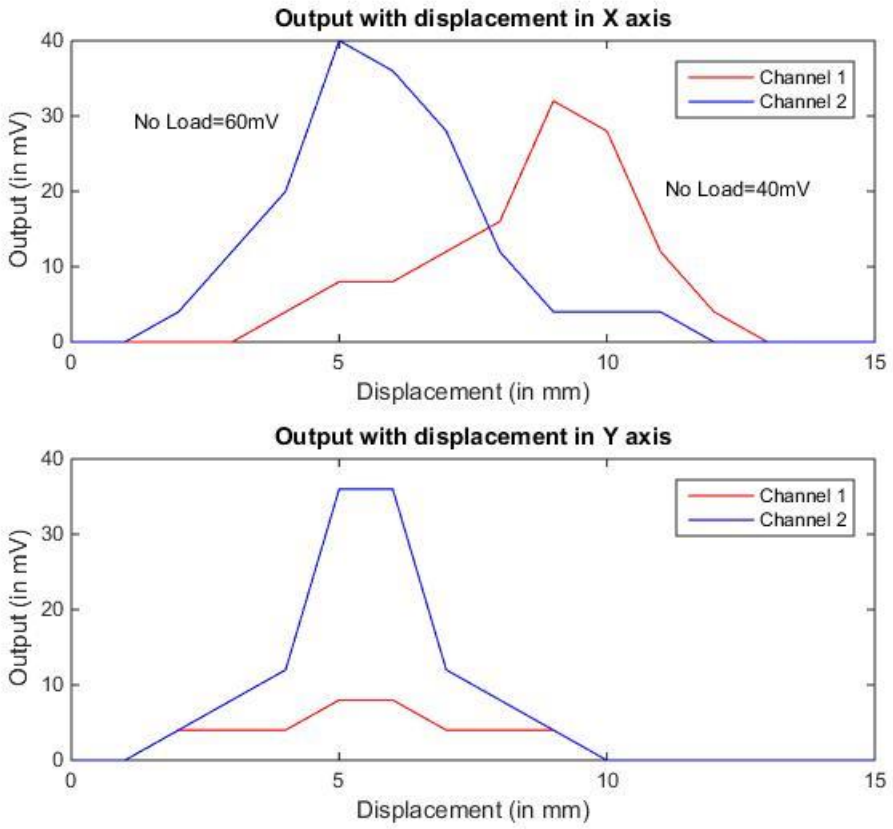


Fig 47: X axis displacement vs Voltage in both channels and Y axis displacement vs Voltage in both channels for a 7mm X 1mm 5 layer parallel interconnect, 2 channel cathodic stimulation PVDF device

Different Z Axis Height

1.25” – 32 mV and 40 mV were the maximum voltages in CH1 and CH 2 respectively

0.86” – 4 mV and 20 mV were the maximum voltages

1.41” – 8 mV and 40 mV were the maximum voltages

4.7.2. PZT Neurostimulators

4.7.2. (i) . Nickel Based Device

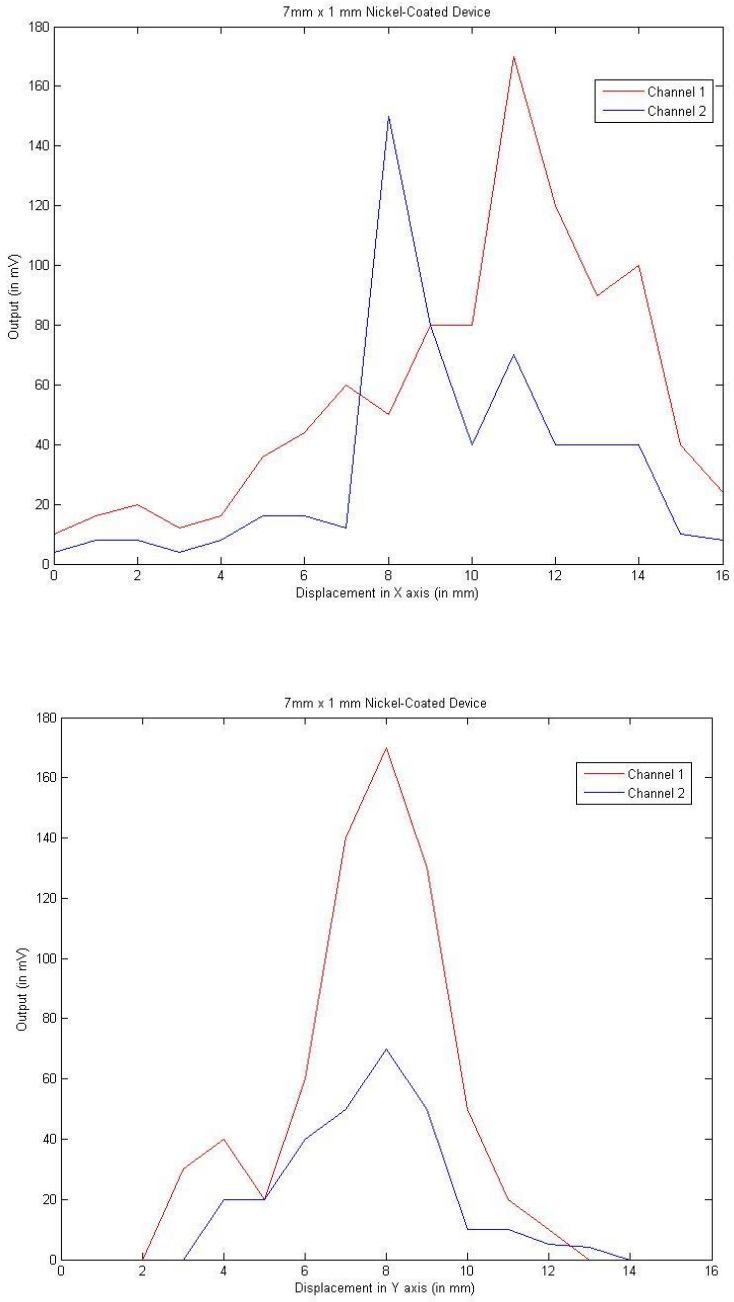


Fig 48: X axis displacement vs Voltage in both channels and Y axis displacement vs Voltage in both channels for a Nickel PZT device

Different Z Axis Height

1.25” – 170 mV and 110 mV were the maximum voltages in CH1 and CH 2 respectively

0.86” – 70 mV and 30mV were the maximum voltages

1.41” – 170 mV and 110 mV were the maximum voltages

Current Produced Against Different Loads

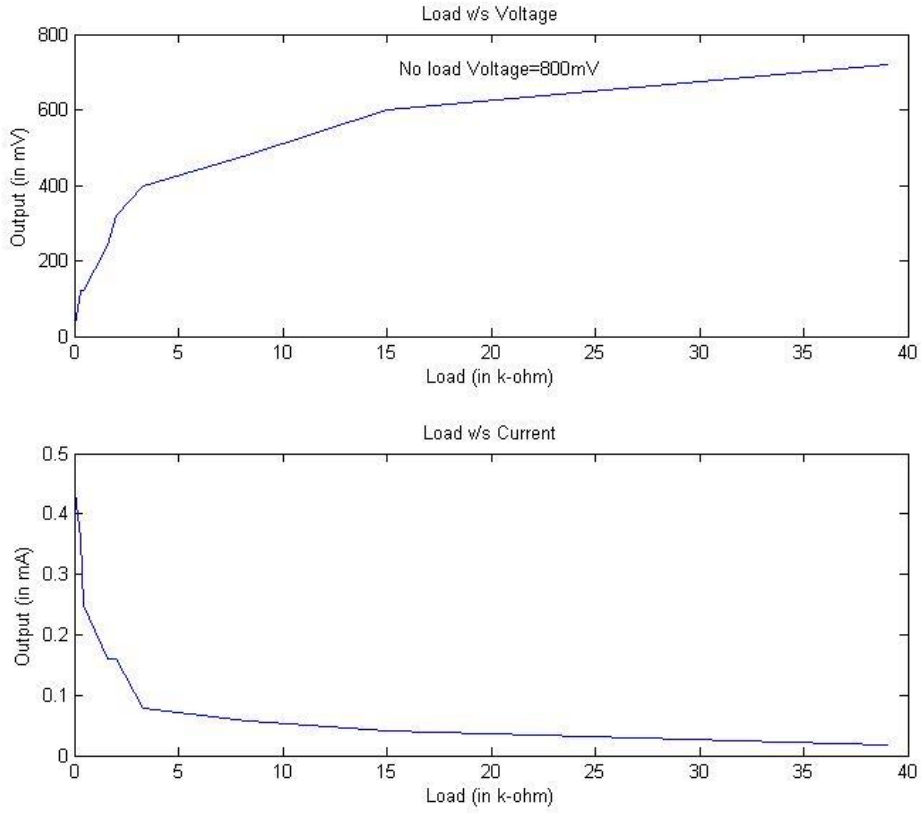


Fig 49: voltage vs load and corresponding current vs load curve determined from the voltage across a given load for Nickel PZT device

4.7.2. (ii). Gold Based Device

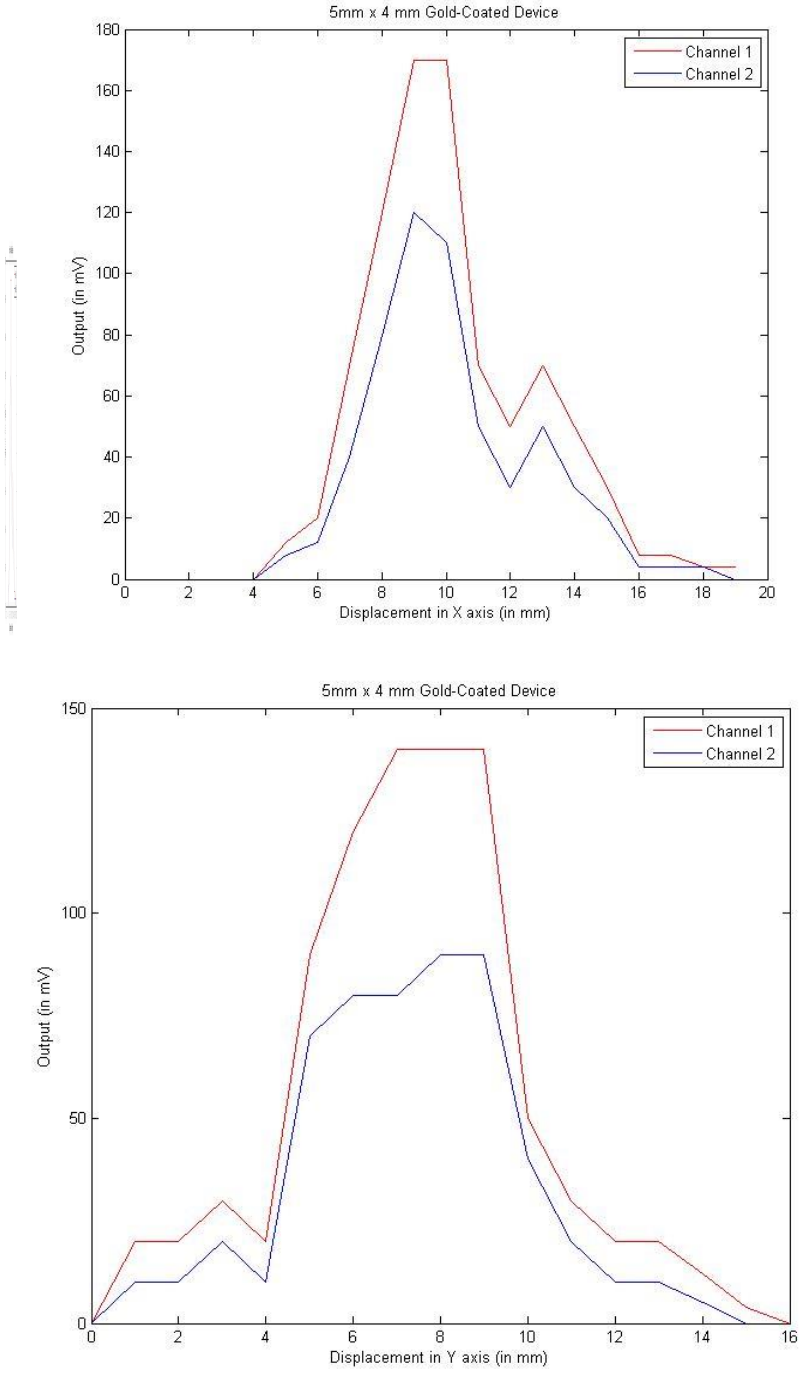


Fig 50: X axis displacement vs Voltage in both channels and Y axis displacement vs Voltage in both channels for a Gold plated PZT device

Different Z Axis Height

1.25” – 170 mV and 110 mV were the maximum voltages in CH1 and CH 2 respectively

0.86” – 60mV and 40 mV were the maximum voltages

1.41” – 180 mV and 110 mV were the maximum voltages

This study proves that the focal depth of the transducer from the surface of the device also plays a major role in determining the output of the device.

Current Produced Against Different Loads

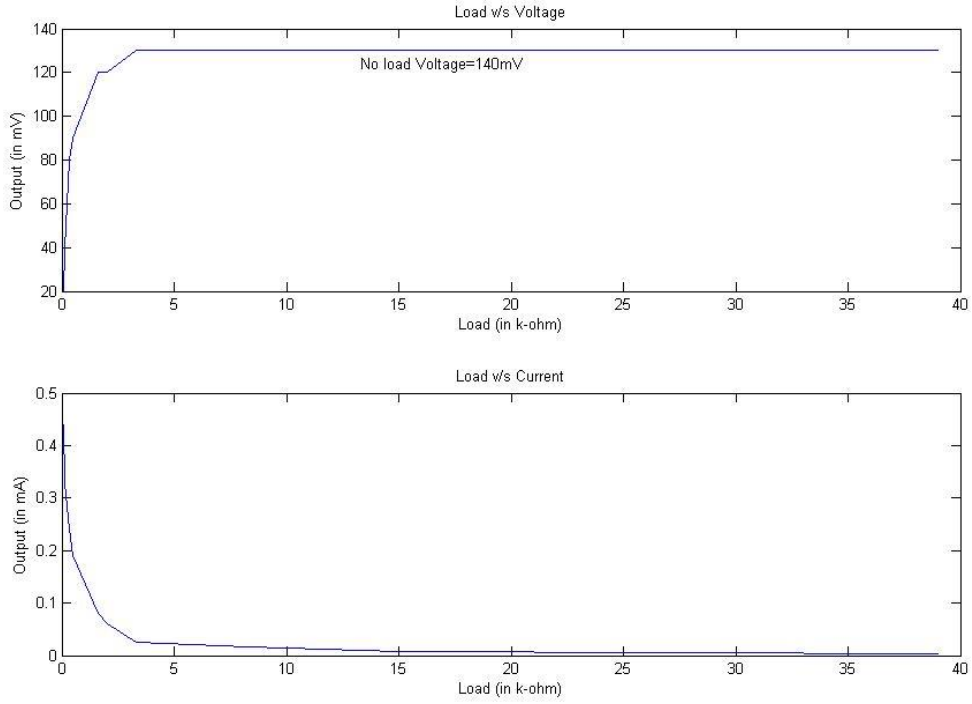


Fig 51: voltage vs load and corresponding current vs load curve determined from the voltage across a given load for Gold coated PZT device

It is to be noted that the voltage drop across different loads varies according to the curve and the current produced accordingly. For neurostimulatory performance of the devices, the load needs to be known and the device can then be driven by the appropriate transducers powered by different voltages that are required to achieve the above discussed effect.

4.8. Output Dependence on Conductivity

4.8.1. PVDF Device

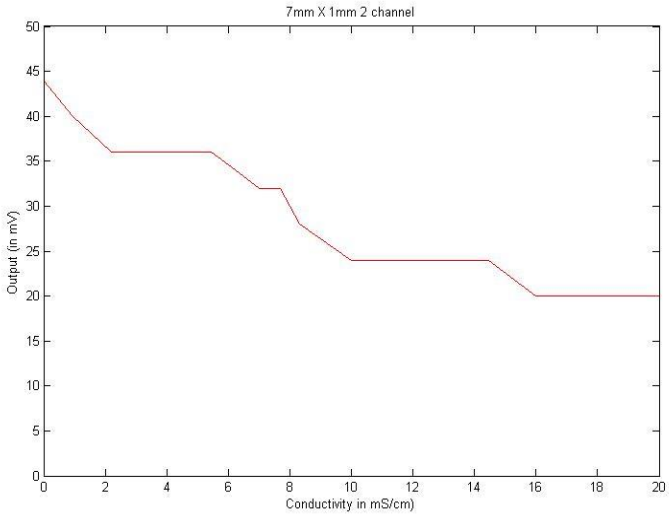


Fig 52: Output dependence on conductivity for a PVDF device

4.8.2. PZT Device

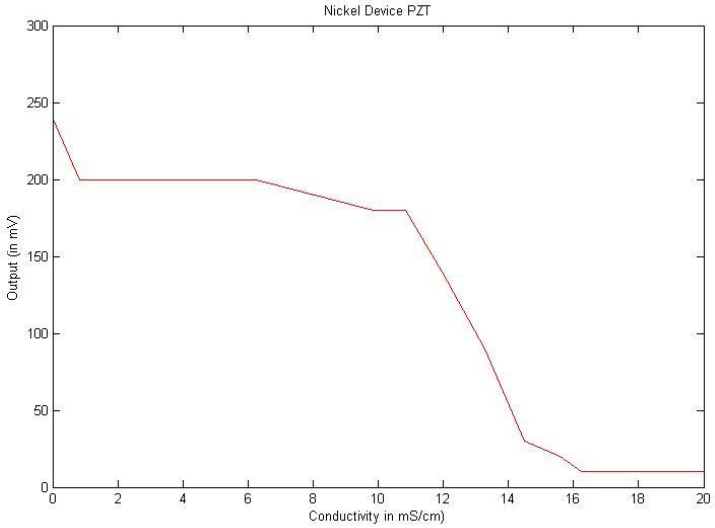


Fig 53: Output dependence on conductivity for a Nickel PZT device

The output is a function of conductivity. At lower conductivities the voltage measured is a maximum followed by a drop and a plateau with increasing conductivities. Our region of interest is in the ranges of 1 – 2 mS/cm as it corresponds to the Brain Gray matter, White matter and nerve

conductivity. The maximum value of 20 mS/cm corresponds to the Cerebrospinal Fluid conductivity which is also similar to a saline solution.

4.9. Impedance Measurements of Different Electrodes: Electrode-Electrolyte Interface

The below plots are bode plots of impedance vs frequency on the log scale. Assuming the frequency to be around 20 Hz, the log of which is 1.3, the corresponding Y axis value is noted and the anti-log of it is calculated to arrive at the impedance values.

4.9.1.

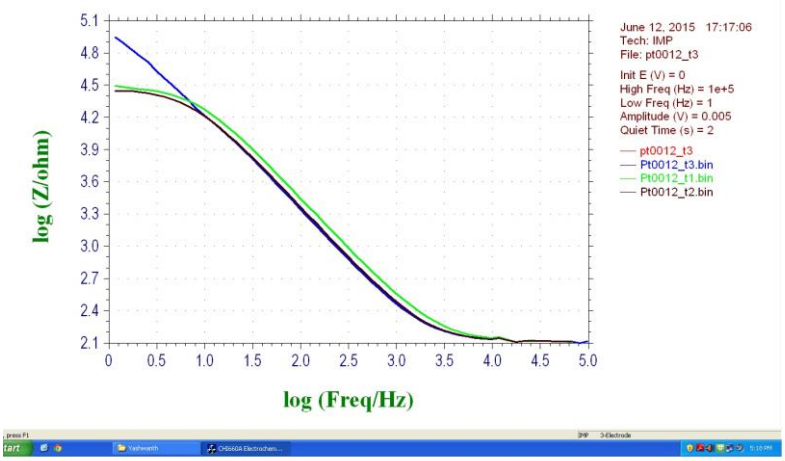


Fig 54: Bode plot of Impedance Vs Frequency on the log scale for a 110um thick PT/IR electrode Teflon coated exposed up to 0.1mm in the solution for 3 iterations

The impedance was measured to be around 15.9 K ohms.

4.9.2.

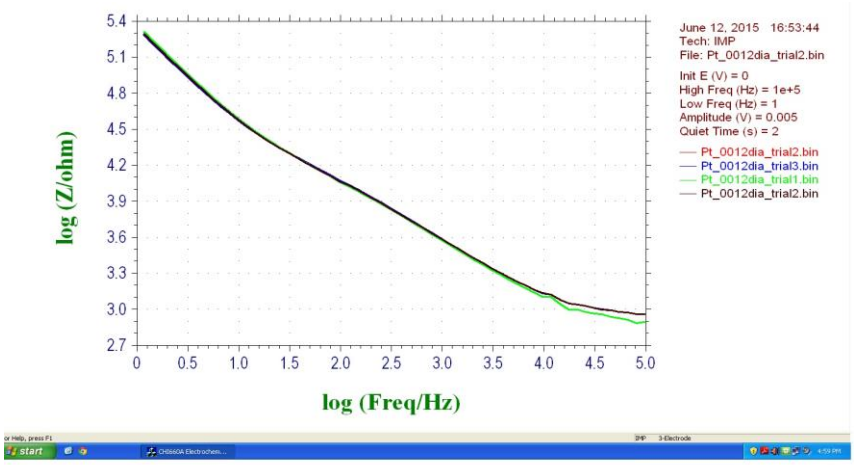


Fig 55: Bode plot of Impedance Vs Frequency on the log scale for a 0.012 inch thick PT/IR electrode exposed up to 5 mm for 3 iterations

The impedance was measured to be around 31.6 K ohms.

4.9.3.

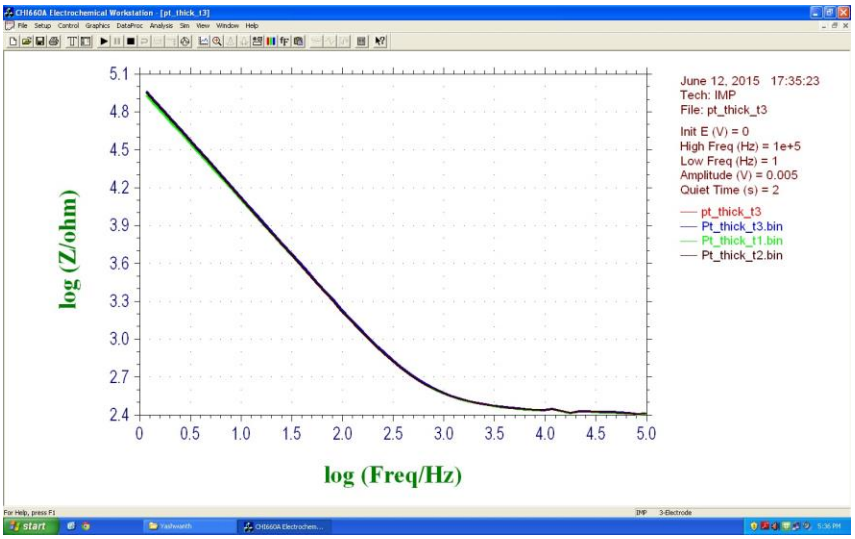


Fig 56: Bode plot of Impedance Vs Frequency on the log scale for a 0.02 inch thick PT/IR electrode exposed up to 5 mm for 3 iterations

The impedance was measured to be around 7.9 K ohms.

4.9.4.

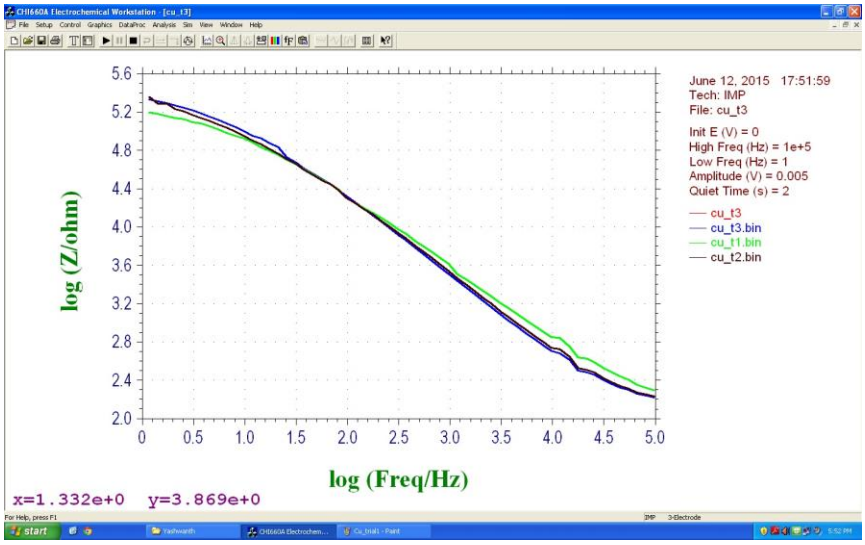


Fig 57: Bode plot of Impedance Vs Frequency on the log scale for a thin copper electrode coated with enamel and the tip scraped and exposed up to 3 mm for 3 iterations

The impedance was measured to be around 63.1 K ohms.

4.9.5.

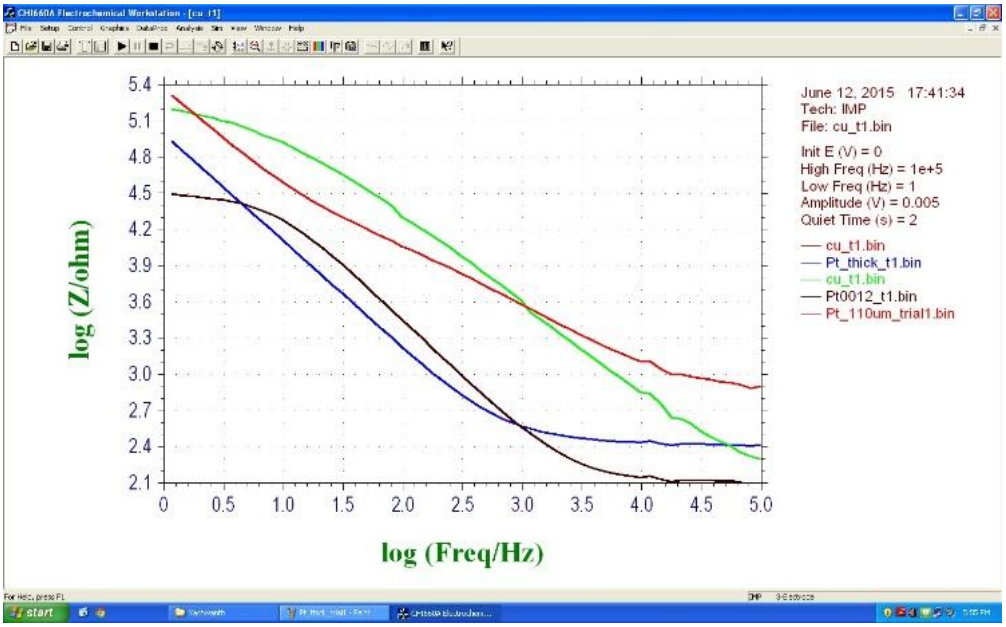


Fig 58: Bode plot summarizing all the electrode plots

4.10. Acoustic Power, Focal Spot and Acoustic Power Density Measurements

The change in mass was found to be 0.008 gms over 4 iterations.

With the focal spot around 0.38 mm^2 [47] the acoustic power density was calculated to be around 305.34 mW/cm^2 which is still less than half of the permissible FDA limits on acoustic power density of the ultrasound waves.

4.11. Wavelengths of the Different Transducers

This is calculated using the formula

Speed of Ultrasound = Freq*Wavelength

The speed is assumed to be 1484 m/s in water

Transducer	Wavelength	Half Wavelength
1 MHz	1.5 mm	0.75 mm
2.25 MHz	0.66mm	0.33 mm
5 MHz	0.3 mm	0.15 mm
20 MHz	0.07 mm	0.035 mm

Table 11: Wavelength and half wavelengths of the different transducers ultrasound beam

This information is crucial, as the device has to be designed in such a way its maximum volume comes under half wavelength of the wave, otherwise it can lead to charge cancellations in the device due to opposite polarity charges developed because of the different parts of the full wave [48].

4.12 Live Animal Experiments

After the successful bench tests the devices, there arose an opportunity to test in several animals for its performance under approved protocols and supervision.

Three different animal species were considered for the tests.

4.12.1. Frog Nerve Experiment

The goal of this experiment was to observe if the device powered by the ultrasound could elicit an action potential in the amphibian nerve. Adult bull frogs were sourced and experiments conducted under an IACUC approval. This is a terminal experiment with the sacrifice of the bull frog. The frog was kept in a container filled with water. About 20mg of MS 222, a powder anesthesia was added to 10 ml of deionized water and the solution was introduced into the container. After about 40 minutes, the frog was checked if it was anesthetized and was taken out of the container. If it wasn't anesthetized, the process was repeated.

Once it is established that the frog is unconscious, it is taken out of the container and placed on the working bench. The frog is pithed using a sharp needle. The frog is turned on its back and the extraction of the sciatic nerve surgically is undertaken. The nerve is extracted from the frog and placed in a petri dish filled with ringer's solution to prevent the nerve from drying up.

The nerve is placed on a platform which had multiple silver electrodes and one end of the nerve extended into the water bath. The setup was similar to the Tone burst setup discussed earlier except that it had an additional external filter to which 2 measuring probes were attached that acted as a differential amplifier and these probes were connected to the Ag/AgCl electrodes on the platform 3cm downstream. These probes had one common negative ground attached to one electrode and the remaining individual positive probes were attached onto either side of this negative probe. The measuring probes were then attached to the CRO (Oscilloscope). The nerve was always kept moist to make sure it didn't dry up by spraying the ringer's solution.

As per the protocol before introducing the device 150 us, bi-phasic electrical stimulus from an AM Systems was used to excite the nerve and the Compound Action Potential (CAP) was recorded.



Fig 59: CAP from the frog nerve

The electrical stimulus electrodes were now replaced by the copper electrodes from the one channel PVDF device. The device was powered by a Linear Power amplifier with the input settings which had 200 us pulses, spaced 2.86 ms apart in bursts of 13 pulses using an isolated current source (AM systems 2100). The bursts were repeated at 1 Hz. Anodal, cathodal, and biphasic pulses were tested, at currents up to 2 mA.

The output from the device was directly connected to the CRO and the output was recorded to measure the device performance as shown in fig.

The electrodes were then introduced into the nerve and the procedure was repeated. Due to high amount of noise a proper CAP signal was not detected as shown in fig and hence this animal study was deemed unfit for future tests.



Fig 60: Device working output (gain of 20dB) and CAP results muffled with noise

4.12.2. Rat Model

Experimental Procedure

The next study involved Sprague-Dawley rats. It was performed in Dr. Kleim's lab. The goal of this experiment was to test the current driving ability of the multichannel electrode system for the purposes of neural stimulation. The protocol had been approved and the following experiments were done according to an IACUC protocol by the researcher approved to perform the surgery and the subsequent steps.

At the beginning of the procedure, the rat was anesthetized with isoflurane (2%) and placed in the stereotax. The skull was exposed. Three drill sites were marked: two were 2-3 mm lateral of bregma, on each hemisphere. The third site was 2-3mm lateral, 5 mm anterior of bregma. Holes were drilled in the skull using a small dremel tool. Then, the anesthesia was switched away from isoflurane, since isoflurane blocks the motor response. The rat was kept anesthetized with ketamine (70 mg/kg, intraperitoneal) and xylazine (5 mg/kg, i.p.).

When the rat began to re-awaken later in the procedure (approximately 1 hour after the first dose), a supplementary half-dose of ketamine (35 mg/kg) was given.

20 minutes after switching to ketamine, a stimulation electrode was inserted through the drill holes (stainless steel wire). Stimulation was applied using a standard ICMS (intracortical microstimulation) protocol [49]: 200 us pulses, spaced 2.86 ms apart in bursts of 13 pulses, using an isolated current source (AM systems 2100). The bursts were repeated at 1 Hz. Anodal, cathodal, and biphasic pulses were tested, at currents up to 3 mA. The ground electrode was tested on the foot, on the scalp, and on the brain (as a bipolar configuration). All 3 drill sites were tested. No brain-evoked motor response could be elicited at any condition.

Because the isolated current source (AM systems 2100) could not evoke a motor response, the preparation was not suitable for testing the ultrasound-powered stimulator. This failure may have been due to variation in the ketamine metabolism, causing the rat to be too deeply anesthetized. It is also possible the cortex was inflamed or damaged in the process of drilling the holes though the skull.

4.12.3. Mice Model

The next set of studies involved studying the performance of these devices in stimulating the mice brain. It was performed in Dr. Muthuswamy's lab under supervision and by a researcher who was approved to perform the experiments. At the beginning of the procedure, the mouse was anesthetized with Ketamine Xylazine Acepromazine given at a scale of 0.1ml/25gm animal weight. The hair on the skull was later removed and the area cleaned before it was placed in the stereotax with a heating pad below and oxygen supply kept at ~1 lpm. The mouse was kept on Isofluorane at ~1 lpm just before the start of the experiment and later in between the experiments it was kept at ~0.5 lpm. The skull was exposed. The burr drill was used to make a craniotomy 3mm anterior and 4 mm posterior to the bregma, and 4 mm lateral to the bregma. Then, the anesthesia was switched away from isoflurane, since isoflurane blocks the motor response.

30 minutes after the shutdown, a stimulation electrode was inserted through the drill holes (Stainless steel) using a micromanipulator driven by a motor to reach 800 um depth. Stimulation was applied using a standard ICMS (intracortical microstimulation) protocol: 200 us pulses, spaced 2.86 ms apart in bursts of 13 pulses using an isolated current source (AM systems 2100). The bursts were repeated at 1 Hz. Cathodal pulses were tested, at currents up to 600 uA. The ground electrode was tested on the foot, on the scalp. Both the drill sites were tested and at different depths ranging from 800 um to 100 um. No brain-evoked motor response could be elicited at any condition.

Because the current source could not evoke a motor response, the preparation was not suitable for testing the ultrasound-powered stimulator. This failure may have been due to the excessive damage to the brain causing by the stimulation electrode and the inefficiency of the stainless steel electrode and possible ground electrode failure.

A second study was performed and the same surgical procedure was performed. The change being instead of a stainless steel electrode, an FHC PT electrode from Micro Probes Inc which has a 1.5 Mohm impedance was used and the ground electrode was attached to the brain skull.

The electrode was introduced into the hole and inserted 800 um deep. The stimulation pulse was similar to the one used in the above experiment. A motor response was seen in the form of the

eyeball bulge, but was termed as an inappropriate response as it was ipsi lateral opposed to a contra lateral response. The preparation was not suitable for testing the ultrasound-powered stimulator. This failure may have been due to the excessive damage to the brain caused by repeated poking of the stimulation electrode and which may have led to a localized stimulation.

A third study was undertaken with the change being a surgical one. The dura was removed to assist with the easy penetration of the electrode to eliminate dips and the ICMS stimulation was performed. A motor evoked response was established in the mouse tail and the right hind limb. This was followed by the placing of the device in the same region using a micromanipulator and pushing the device to a depth of 800 um. A thin layer of coupling gel was introduced on top of the device and a custom made funnel with a parafilm coating at the short end was place on top of the gel to couple with device and filled with distilled water. The transducer was then placed in the water with a Z axis fixed at 1.25” from the surface of the device to provide an effective coupling medium for the ultrasound waves to the device. The transducer was attached to the custom micromanipulator built and in turn attached to a Linear Power amplifier. It is powered by the same pulses as the ICMS except that the pulse now had been modulated with a resonant frequency signal that of the transducer.

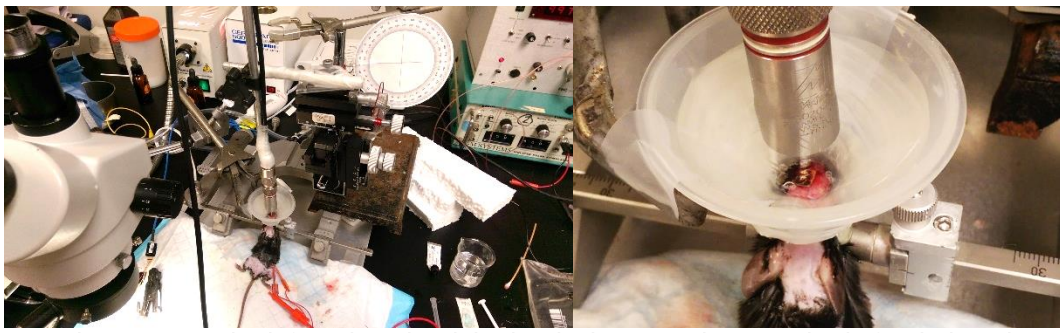


Fig 61: The setup on the left and on the right the device was photographed after being placed in the brain

The micromanipulator was now moved in the X and Y axis to activate the channels. However, no motor evoked response was seen. This might have been due to the damage to the brain as it was 10 hours into the procedure and the outage of oxygen supply in between the study.

This animal study was also deemed unfit as the mouse brain was too fragile to be poked multiple times at the same region to see an ICMS response by a stimulating electrode followed by the introduction of the device and then performing the experiment again.

CHAPTER 5

DISCUSSION

Potentially implantable miniature medical devices are considered in this work as an alternative to the traditional wired stimulators. An ideal multichannel device needs to be compact, mechanically stable, and biocompatible and produce DC neuro stimulatory output.

This work investigated the design, construction and tested the performance of polyvinylidene fluoride and lead zirconate titanate devices as methods of converting ultrasound energy to electrical energy and the potential implantables.

A quick summary the two sets of devices.

PVDF Neurostimulator:-

Advantages:

- Known to be biocompatible and Flexible.
- Clear distinction of the two channels.
- Multiple channels in series interconnects were accomplished more compactly. Up to 4 channel devices were constructed.
- Parallel interconnect devices were constructed to have better output port impedances in the range of the tissue.

Disadvantages:

- Takes longer times to manufacture due to the low thermal tolerance. Any temperature rise beyond 80^{o}C can lead to depolarization of the PVDF.
- Unable to create more than 2 channel in parallel interconnects. They can be created, but will be bulkier.
- At the ultrasound power levels tested PVDF produced insufficient voltage to exceed diode threshold and was not furthered considered

PZT Neurostimulator:-

Advantages:

- Practically faster to manufacture using novel laser cutting procedure.
- Laser cuts make the channels more precise.
- Up to 2 channel devices were constructed and designs of 6 channel devices (a snow flake) were constructed

Disadvantages

- Laser cuts for prolonged iterations on thicker materials made the devices brittle.
- Thinner devices weren't mechanically stable and thicker devices couldn't be cut with the current laser
- The devices had an internal acoustic transfer of energy causing both the channels to be active, but they were still distinct due to its peaking of voltages at different times.

Design of the Multichannel Stimulators

5.3. Fabrication of PVDF Devices

5.3.1. Need for Series and Parallel Devices

A 5 layer was chosen as the norm to construct the devices with series interconnects. As the series devices were constructed, as it provided more flexibility in making multiple channels, it was noticed that these devices had lower capacitances, which in turn meant that the output port impedances were really high and hence provided very poor transfer of charge generated, to the tissue. Hence parallel interconnects were constructed as it had lower output port impedances, the trade-off being a little bit more bulkier devices.

Also, one factor that was taken into consideration as we went into further animal tests was the need to make really compact devices and hence a 3 layer device was constructed and its performance was evaluated against a 5 layer device and tested using a 2.25 MHz transducer. The 3 layer device showed a better output and it was established that it was due to the half wavelength of the ultrasound beam from the transducer which was around 6mm. Hence the 4^{th} layer and 5^{th}

layer in a 5 layer device produced negative charge of opposite polarity that caused a cancellation of charge and lead to lesser output.

5.3.2. Cathodic and Anodic Stimulation

Initially devices mostly anodic stimulation devices were built to show the multichannel functionality. However on seeing substantial results in the initial bench tests it was established the need to construct Cathodic stimulation devices which is the norm for neural stimulation.

5.4. Fabrication of PZT Devices

Several designs were created before the final design was finalized. The initial designs involved cutting a PZT base using laser cutter with holes punched by the laser for the diode connections to be made. The nickel metal layer was removed and replaced with gold. This didn't create the perfect channels and hence a laser cut method was chosen to partially scrape the top layers with which we can make distinct channels. This method meant we could employ any design on the PZT using the laser cutting machine with ease and precision. For an ideal PZT device, for a 2 channel a rectangular design and for a 6 channel a snow flake design was envisioned.

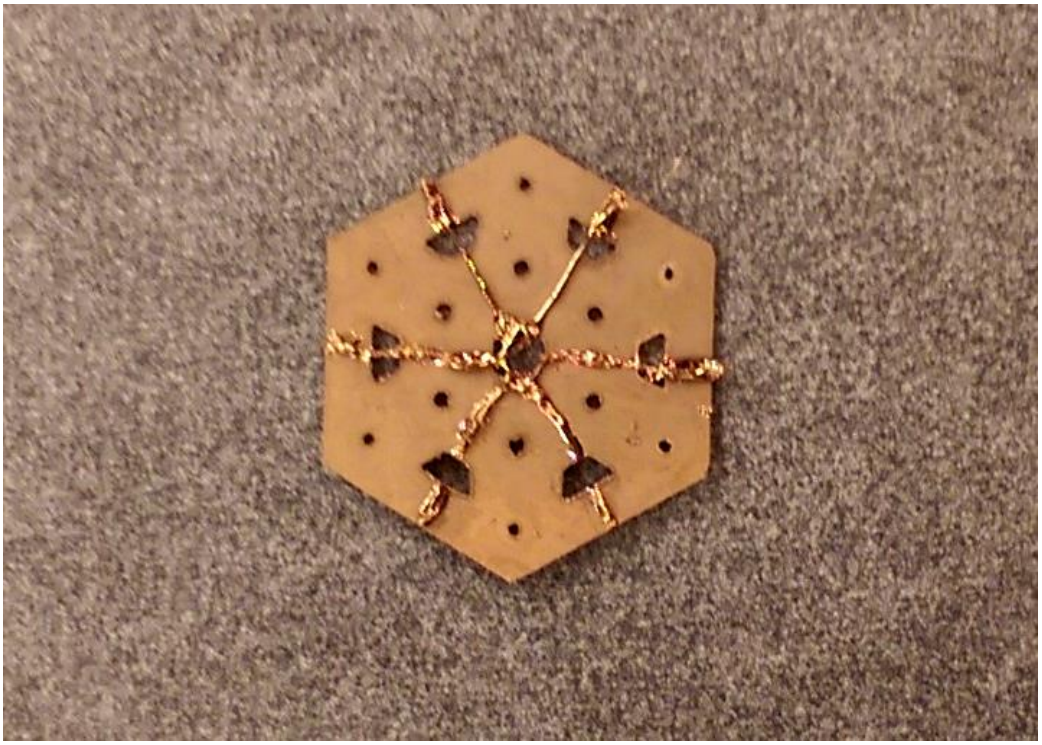


Fig 62: A honeycomb structure for a 6 channel gold plated PZT based device.

A honey comb structure was designed to make the device more mechanically stable with several spaces as shown above created to increase the acoustic isolation between the channels and the holes for creating the connects with the diode.

5.4.1. Need for Gold Plated And Nickel Plated Devices

Gold plated devices were ideal as they provided better biocompatibility. However since fine channel separations couldn't be made, a nickel based device with laser cut channels was made.

However, Nickel devices corrode quickly in conductive solutions. Therefore the better option would be constructing a laser cut nickel device with the return electrode side coated with gold as the other side is already encapsulated in biocompatible non-conductive epoxy to increase the biocompatibility of these devices.

General Considerations for future designs:

Series connection of diodes and also the use of die based packages can substantially reduce the size of devices and also increases the possibility of increasing the number of channels closely spaced making it more compact.

5.5.2 .Multichannel Capability in PVDF and PZT Devices

The multichannel capability was established in the PVDF and as well as PZT devices up to 2 channels.

In PVDF devices, the 2 channels worked very distinctly, meaning when one channel was active, the other channel was completely inactive. This is due to the fact of it being a plastic material and less crystallinity and hence there was no acoustic transfer of power through the material. However in PVDF devices more than 2 channel devices didn't perform practically as expected from a theoretical standpoint due to the fact that the channel spacing was too low and also some of the channels were depolarized due to the solder.

One other observation at the end of this study was that all the diodes were parallel attached. However recent studies showed that a series connection would also be an apt choice to make the devices. This provides scope for much more compact devices to be manufactured. Future multichannel devices could employ this design and its efficiency could be tested out against the current devices to establish the better design out of both the possibilities.

Even though PVDF devices showed better multichannel capability, they did not produce enough voltage to get rectified by the diode to generate a DC output and hence did not evoke the ICMS required.

PZT devices were found to produce an ample voltage for the diode to get rectified and produce a DC voltage and current that is neuro stimulatory. However, the distinction between the channels has been of lower resolution. This is due to the fact that PZT is a highly crystalline structure and hence there was an acoustic transfer of power within the crystal. But when the Current vs Load plot is taken (mention plot), it clearly shows that it produces sufficient current at a particular

voltages which are the peaks for the two channels, hence these act as distinct channels that evoke a possible response in the two different regions of the brain.

5.6. Animal Experiments

The animal experiments were pursued to get a better understanding of the device performance. The rat and mouse experiments were performed on an existing protocol which mandated those experiments already on the protocols be performed first and then paved way for the devices to be tested. This often lead to longer wait times, which meant the brain lost substantial functionality or was damaged too much to evoke a motor response.

Future animal studies would require the establishment of protocols and overcome the severe limitations faced in terms of making low impedance electrodes matching that of the tissue and that would penetrate the brain only till the 5^{th} layer, to reach the motor cortex.

CHAPTER 6

CONCLUSION

This work has evaluated the performance of a novel multichannel neural stimulator constructed out of Polyvinylidene Fluoride (PVDF) polymer and Lead Zirconate Titanate ceramic and powered by ultrasound for the purpose of Intracortical microstimulation. This can be later expanded to other applications that can include in the study of treatment of epilepsy, and in deep brain stimulation.

PVDF devices didn't show neurostimulatory output but had better channel differentiation. PZT devices produced neurostimulatory output that could evoke a response in the mouse brain.

Series interconnects of PVDF with diodes in series connection or potentially replaced with die packages can be an alternative to make more compact devices. And with the use of diodes that have lesser bias voltages, a DC neuro stimulatory output can be created. High g_{ij} value PVDF materials can also be considered.

PZT devices were made to host more than one channel. Up to 6 channels were envisioned in this thesis work. The snow flake design brings more mechanical stability and also the spaces bring distinction and acoustic separation between the various closely spaced channels. Additional work needs to be carried out to make devices that can host multiple channels, more than six in a compact space similar to that of integrated chips. Thicker devices for higher can also be constructed by using high power laser cutter to make precise cuts and channels.

In-vivo experiments in animal model could not be performed effectively due to unfavorable conditions. Future studies need to focus on the improvement of the in-vivo experimental model and creating a new protocol to further carry out this study to strongly establish these devices as an alternative to the traditional wired stimulators.

REFERENCES

[1] Hsu K H et al 2003 Analysis of efficiency of magnetic stimulation IEEE Trans. Biomed. Eng. 50 1276–85

[2] Yoo S S et al 2011 Focused ultrasound modulates region-specific brain activity NeuroImage 56 1267 – 75

[3] Hannan M.A., Mutashar S., Samad S.A., Hussain A. (2014). “Energy harvesting for the implantable biomedical devices: issues and challenges,” BioMedical Engineering OnLine, 13:79.

[4] Sahin M., Pikov V. (2011). “Wireless microstimulators for neural prosthetics”. Crit. Rev. Biomed. Eng. 39 63–77 10.1615/CritRevBiomedEng.v39.i1.50.

[5] Wells J et al 2005 Optical stimulation of neural tissue in vivo Opt. Lett. 30 504–6

[6] Schulman., “The Feasible FES System: Battery Powered BION stimulator”, 1226 – 1227

[7] Boon P, Raedt R, Herdt V, Wyckhuys T, Vonck T, “Electrical Stimulation for the treatment of epilepsy”, Vol. 6, 218 – 227, April 2009, The American Society for Experimental NeuroTherapeutics, Inc.

[8] Hodaie M, Wennberg RA, Dostrovsky JO, Lozano AM. Chronic anterior thalamus stimulation for intractable epilepsy. Epilepsia 2002; 43:603– 608.

[9] McCreery D, Lossinsky A, Pikov V, Liu X, “Microelectrode array for chronic Deep-Brain Microstimulation and recording”, 726 - 737, 2006, IEEE

[10] E. B. Montgomery Jr., “Deep brain stimulation for hyperkinetic disorders,” Neurosurg. Focus., vol. 17, p. E1, 2004.

[11] C. C. McIntyre, M. Savasta, B. L. Walter, and J. L. Vitek, “How does deep brain stimulation work? Present understanding and future questions,” J. Clin. Neurophysiol., vol. 21, pp. 40–50, 2004.

[12] Sanguineti V et.al, “Neuro –Engineering: from neural interfaces to biological computers”, 2003

[13] Phillips CA, Hendershot DM. Functional electrical stimulation and reciprocating gait orthosis for ambulation exercise in a tetraplegic patient: a case study. Paraplegia 29 (4) (1991) 268-76.

[14] Rabischong E, Ohanna F. Effects of functional electrical stimulation (FES) on evoked muscular output in paraplegic quadriceps muscle. Paraplegia 30 (7) (1992) 467-73.

[15] Rabischong P. Modern techniques of restoration of locomotion in paralyzed persons. Bull Acad Natl 183 (3) Med (1999) 531-7.

[16] Biering-Sorensen F, Gregersen H, Hagen E, Haugland M, Keith M, Larsen CF, Leicht BP, Nielsen FH, Rabischong E, Sinkjaer T. Improved function of the hand in persons with tetraplegia using electric stimulation via implanted electrodes. Ugeskr Laeger 10, 162(15) (2000) 2195-8.

[17] Branner A, Normann R, “ A multielctrode array for intrafascicular recording and stimulation in sciatic nerve of cats”, 1999

[18] A. Branner, R.B. Stein, E. Fernandez, Y. Aoyagi, R.A. Normann, Long-term stimulation and recording with a penetrating microelectrode array in cat sciatic nerve IEEE Trans. Biomed. Eng. 51, 146–157 (2004). doi:10.1109/TBME.2003.820321

[19] P.K. Campbell, K.E. Jones, R.J. Huber, K.W. Horch, R.A. Normann, A silicon-based, three-dimensional neural interface: manufacturing processes for an intra cortical electrode array IEEE Trans. Biomed. Eng 38, 758–768 (1991). doi:10.1109/10.83588

[20] K.E. Jones, P.K. Campbell, R.A. Normann, A glass/silicon composite intra cortical electrode array Ann. Biomed. Eng. 20, 423–437 (1992). doi:10.1007/BF02368134

[21] P.J. Rousche, R.A. Normann, Chronic recording capability of the Utah Intracortical Electrode Array in cat sensory cortex J. Neurosci. Methods 82, 1–15 (1998). doi:10.1016/S0165-0270 (98)00031-4

[22] Larson, Patrick J., and Bruce C. Towe. "Miniature ultrasonically powered wireless nerve cuff stimulator." Neural Engineering (NER), 2011 5th International IEEE/EMBS Conference on. IEEE, 2011.

[23] G. E. Loeb, R. A. Peck, W. H. Moore and K. Hood (2001). "BION™ system for distr. neuralprosthetics," Med. Eng. Phys., vol. 23, pp. 9-18, 1.

[24] Abdo A., Ersen A., Sahin M. (2013). “Near-infrared light penetration profile in the rodent brain”. J Biomed Opt 18:075001.

[25] Denisov A. and Yeatman E. (2010). "Ultrasonic vs. inductive power delivery for miniature biomedical implants," in Body Sensor Networks (BSN), 2010 International Conference on, pp. 84-89.

[26] Biederman, W.; Yeager, D.J.; Narevsky, N.; Koralek, A.C.; Carmena, J.M.; Alon, E.; Rabaey, J.M. (2013). "A Fully-Integrated, Miniaturized (0.125 mm²) 10.5 μW Wireless Neural Sensor," Solid-State Circuits, IEEE Journal of , vol.48, no.4, pp.960,970.

[27] Rabaey, J.M.; Mark, M.; Chen, D.; Sutardja, C.; Chongxuan Tang; Gowda, S.; Wagner, M.; Werthimer, D. (2011). "Powering and communicating with mm-size implants," Design, Automation & Test in Europe Conference & Exhibition (DATE), 2011, vol., no., pp.1,6

[28] Becerra-Fajardo L., Ivorra A. (2014). "Towards Addressable Wireless Microstimulators Based on Electronic Rectification of Epidermically Applied Currents". International IEEE/EMBS Conference.

[29] Sodagar A.M., Amiri P. (2009). “Capacitive coupling for power and data telemetry to implantable biomedical microsystems”. IEEE EMBS 2009 Conf 411-4.

[30] Clark GM. Cochlear implants: fundamentals and applications. New York: Springer-Verlag; 2003.

[31] Abdo A., Sahin M., Freedman D.S., Cevik E., Spuhler P.S., Unlu M.S. (2011b). “Floating light-activated microelectrical stimulators tested in the rat spinal cord”. J Neural Eng 8:056012.

[32] Towe, Bruce C. "Passive backscatter biotelemetry for neural interfacing." Neural Engineering, 2007. CNE'07. 3rd International IEEE/EMBS Conference on. IEEE, 2007.

[33] Arra, Satu, et al. "Ultrasonic power and data link for wireless implantable applications." Wireless Pervasive Computing, 2007. ISWPC'07. 2nd International Symposium on. IEEE, 2007.

[34] Phillips, W. B., B. C. Towe, and P. J. Larson. "An ultrasonically-driven piezoelectric neural stimulator." Engineering in Medicine and Biology Society, 2003. Proceedings of the 25th Annual International Conference of the IEEE. Vol. 2. IEEE, 2003.

[35] Vázquez Carazo, Alfredo. "Novel piezoelectric transducers for high voltage measurements." (2000).

[36] "Interfacing Piezo Film to Electronics." Measurement Specialties. March 2006. Retrieved December 2, 2007

[37] Ozeri, Shaul, and Doron Shmilovitz. "Ultrasonic transcutaneous energy transfer for powering implanted devices." Ultrasonics 50.6 (2010): 556-566

[38] Kawanabe, Hideyuki, et al. "Power and information transmission to implanted medical device using ultrasonic." Japanese journal of applied physics 40.5S (2001): 3865.

[39] Shih, Wen-Pin, and Wen-Pin Shih. "Design, fabrication, and application of bio-implantable acoustic power transmission." Microelectromechanical Systems, Journal of 19.3 (2010): 494-502.

[40] Uchino, Kenji. Introduction to piezoelectric actuators and transducers. PENNSYLVANIA STATE UNIV UNIVERSITY PARK, 2003.

[41] Piezo System, Inc. “Introduction to Piezoelectricity”

[42] Zong, “Applications of Miniaturized Ultrasound Powered Wireless Nerve Stimulators for Pain Management”, Arizona State University 2014, 9 – 10.

[43] Gulick D., Towe B, “Characterization of Simple Wireless Neurostimulators and Sensors”, 2014, IEEE

[44] Calculation of the Dielectric Properties of Body Tissues in the frequency range 10 Hz - 100 GHz http://niremf.ifac.cnr.it/ , 2015

[45] Jaksukam K., Umchid S., “Development of Ultrasonic Power Measurement Standards in Thailand”, ICEMI 2011,

[46] Chen K et.al, “The effect of chronic intracortical microstimulation on the electrode- tissue interface”, 2014

[47] Celinskis D., “Investigation of Ultrasonically Powered Implantable Microdevices for wWireless Tissue Impedance Measurements”, Arizona State University, 2015

[48] Speed of Ultrasound, http://www.wikiecho.org/wiki/Physics_of_ultrasound, 2015

[49] Kleim JA1, Barbay S, Nudo RJ. “Functional reorganization of the rat motor cortex following motor skill learning.” J Neurophysiol. 1998 Dec;80(6):3321-5.

[50] Hao Jiang, Jun Min Zhang, Shy Shenq Liou, Fechter, R., Hirose, S., Harrison, M., Roy, S.(2010). "A high-power versatile wireless power transfer for biomedical implants," Engineering in Medicine and Biology Society (EMBC), 2010 Annual International Conference of the IEEE , vol., no., pp.6437,6440.